

Supporting Information

Structural Isomerism Leading to Variable Proton Conductivity in Indium (III) Isophthalic Acid Based Frameworks

Tamas Panda, Tanay Kundu, and Rahul Banerjee*

*Physical/Materials Chemistry Division, CSIR National Chemical Laboratory, Dr. Homi
Bhabha Road, Pune-411008, India.*

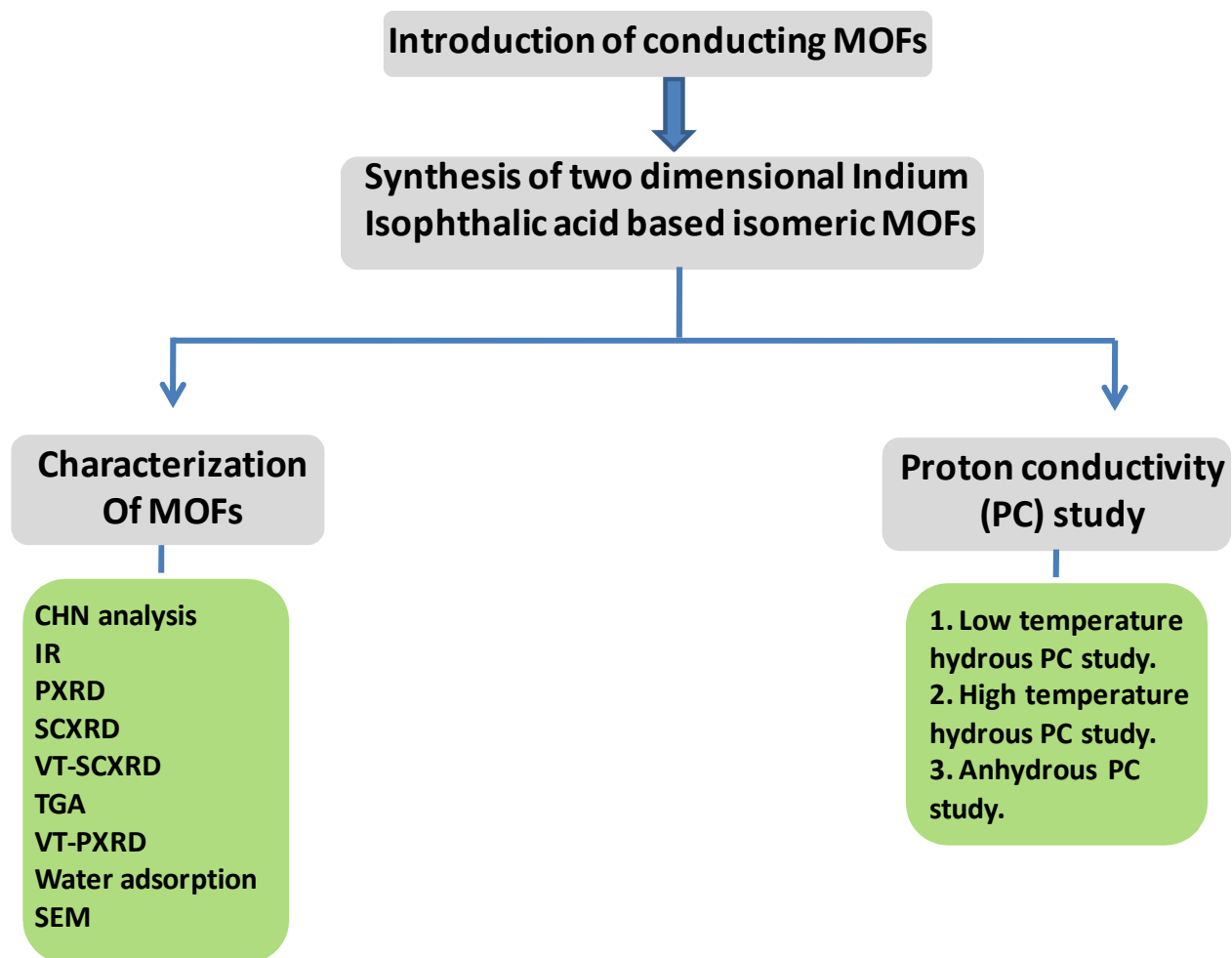
E-mail: r.banerjee@ncl.res.in Fax: + 91-20-25902636; Tel: + 91-20-25902535

CONTENT

Section S1. Detailed synthetic procedures, PXRD patterns and IR spectra for In-IA-2D-1 and In-IA-2D-2 based MOFs	3-6
Section S2. Single crystal X-ray diffraction data collection, structure solution and refinement procedures.	7-16
Section S3. TGA data and the thermal stability of In-IA-2D-1 and -2 MOFs.	17-21
Section S4. Single crystal structures of In-IA-2D-1 and -2 MOFs	22-25
Section S5. Water vapor adsorptions of In-IA-2D-1 and -2 MOFs	26-28
Section S6. Proton conductivity studies of In-IA-2D-1 and -2 MOFs.	29-40
Section S7. Solid state NMR and I-V profile	41

Information flow

This manuscript and the consequent supporting information have been prepared according to the order shown.



Section S1. Detailed synthesis procedures of MOFs including multi-gram scale products, experimental and simulated PXRD patterns:

All reagents and solvents for synthesis and analysis were commercially available and used as received. The Fourier transform (FT) IR spectra (KBr pellet) were taken on a *BRUKER FT-IR SPECTRUM* (Nicolet) spectrometer. Powder X-ray diffraction (PXRD) patterns were recorded on a Phillips PANalytical diffractometer for Cu K α radiation ($\lambda = 1.5406 \text{ \AA}$), with a scan speed of 2° min^{-1} and a step size of 0.02° in 2θ . Thermo-gravimetric experiments (TGA) were carried out in the temperature range of 25–800 °C on a SDT Q600 TG-DTA analyzer under N₂ atmosphere at a heating rate of $10^\circ \text{ C min}^{-1}$. Isophthalic acid and Indium nitrate Hydrate were purchased from the Aldrich Chemicals. All starting materials were used without further purification. All experimental operations were performed in air.

Synthesis of In-IA-2D-1 [In(IA)₂ {(CH₃)₂NH₂} (H₂O)₂]: In the synthesis of In-IA-2D-1, we used isophthalic acid (IA) as organic linker and In(NO₃)₃.xH₂O as a metal salt. Solvothermal reaction between 1.0 mmol of IA (0.170 gm), 1.00 mmol of tetramethylammonium chloride (0.1096 gm) and 0.3 mmol of In(NO₃)₃.xH₂O (0.102 gm) in 4 ml N,N'-dimethylformamide (DMF) and 1 ml H₂O kept at 120 °C for 96 hours yielded rod shaped crystals of In-IA-2D-1 MOF.

FT-IR: (KBr 4000-600 cm⁻¹): 2977 (w), 2307(w), 2172 (w), 1679 (w), 1610 (m), 1550(m), 1486(w), 1374(d,s), 1163(w), 1069(w), 992(w), 852(w), 793(w), 739(s), 657(m), cm⁻¹.

Elemental analysis (%) of as synthesized sample [In(IA)₂ {(CH₃)₂NH₂}(H₂O)₂] calcd: C (44.83%), H (4.12%), N (4.98%); **Found:** C (44.75%), H (4.21%), N (5.08%)

Elemental analysis (%) of vacuum dried sample [In(IA)₂ {(CH₃)₂NH₂}] calcd: C=41.14%, H=3.84 % and N=2.66%; **Found:** C=41.2%, H=3.91% and N=2.62%

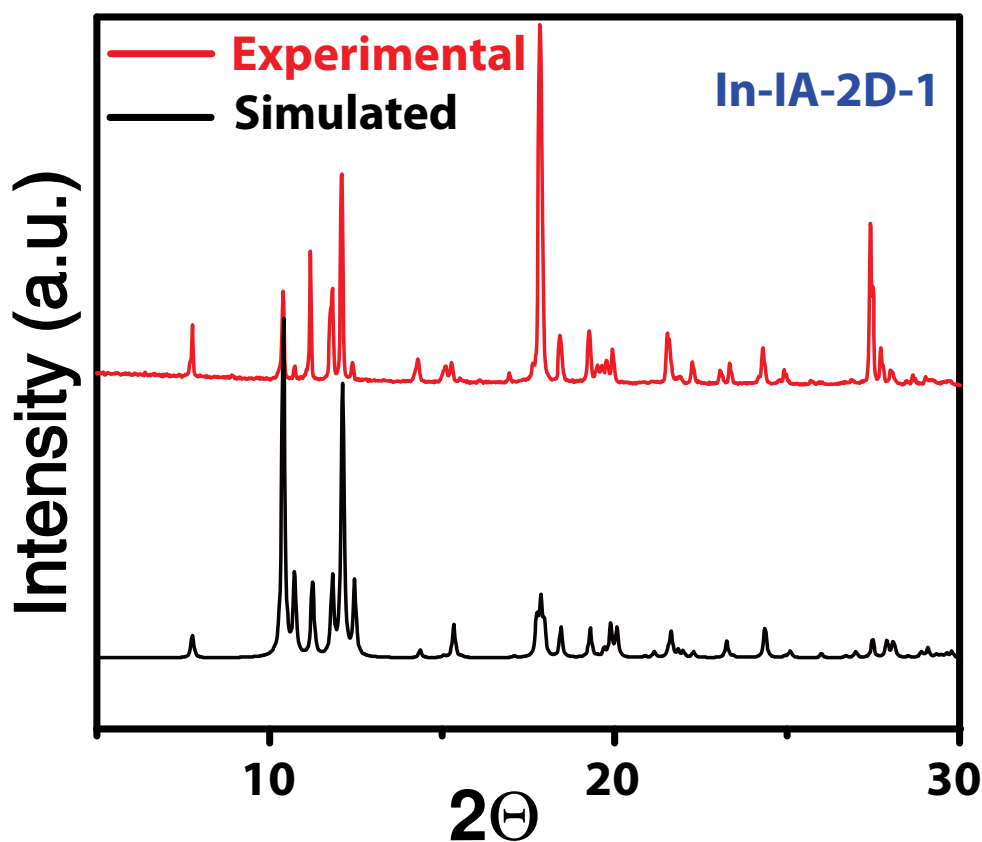


Figure S1. Comparison of the experimental PXRD pattern of as-synthesized In-IA-2D-1 (top) with the simulated one from its single crystal structure (bottom).

Synthesis of In-IA-2D-2 [$\text{In}(\text{IA})_2\{(\text{CH}_3)_2\text{NH}_2\}(\text{DMF})$]: 0.3 mmol of IA (0.049 gm) and 0.1 mmol of $\text{In}(\text{NO}_3)_3 \cdot 3\text{H}_2\text{O}$ (0.031 gm) were taken in a 15 ml scintillation vial. A mixture of 2 ml of DMF and 1 ml of H_2O was added and sonicated for 30 minutes, then transferred to a pre-heated oven at 90 °C for 126 hours. Cube shaped crystals of In-IA-2D-2 was filtered washed repeatedly with DMF and H_2O and air dried for 20 minutes (yield~ 77%).

FT-IR: (KBr 4000-600 cm^{-1}): 2319(w), 1668(m), 1610(m), 1526(s), 1350(d, s), 1163(w), 1080(m), 1022(w), 928(w), 840(m), 746(s), 657(m) cm^{-1} .

Elemental analysis (%) calcd: C (34.37%), H (3.90%), N (7.29%); Found C (34.35%), H (3.92%), N (7.25%).

Note: It should be noted that, during the synthesis of In-IA-2D-2, we have not used any tetramethyl ammonium chloride salt. However, in the crystal structure of In-IA-2D-2, dimethylammoniumchloride cations are trapped inside the framework. The origin of dimethyl ammonium cation within the anionic framework occurs via In(III) metal mediated hydrolysis of DMF molecules^{1,2} under solvothermal condition

References:

1. Papaefstathiou, G. S.; Manessi, S.; Raptopoulou, C. P.; Behrman, E. J.; Zafiropoulos, T. F. *Inorg. Chem. Commun.* 2004, **7**, 69.
2. Tsuchimoto, M. Yoshioka, N. Ohba, S. *Eur. J. Inorg. Chem.* 2001, 1045

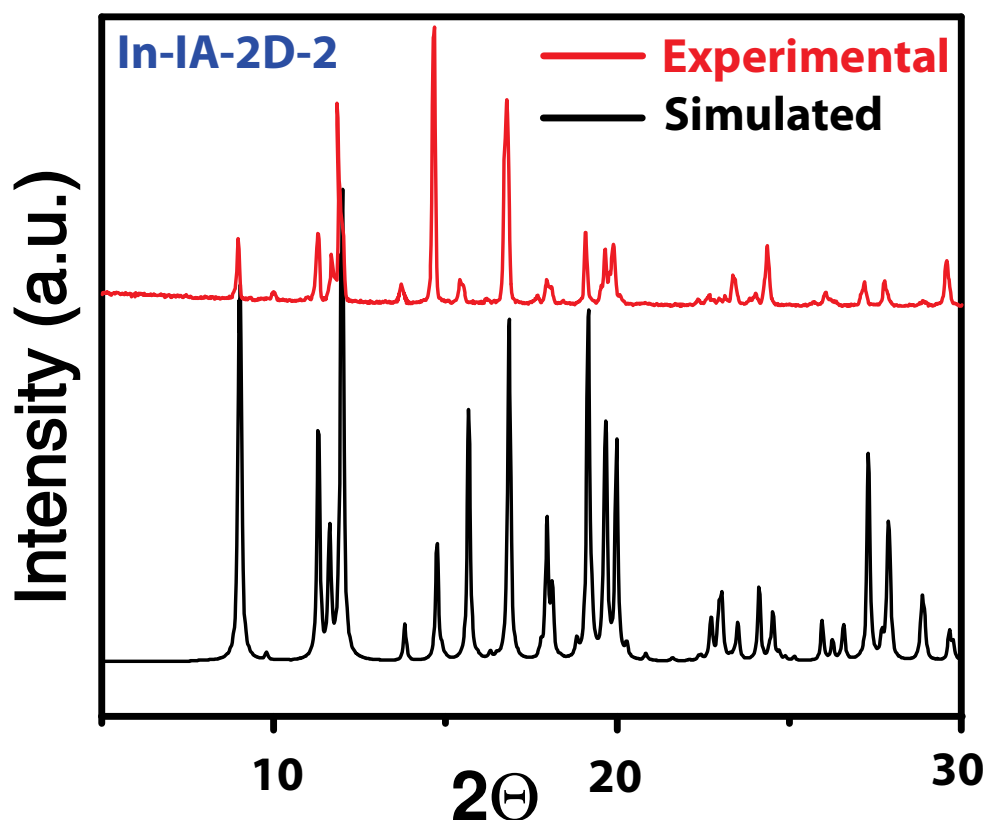


Figure S2. Comparison of the experimental PXRD pattern of as-synthesized In-IA-2D-2 (top) with the simulated one from its single crystal structure (bottom).

IR spectra:

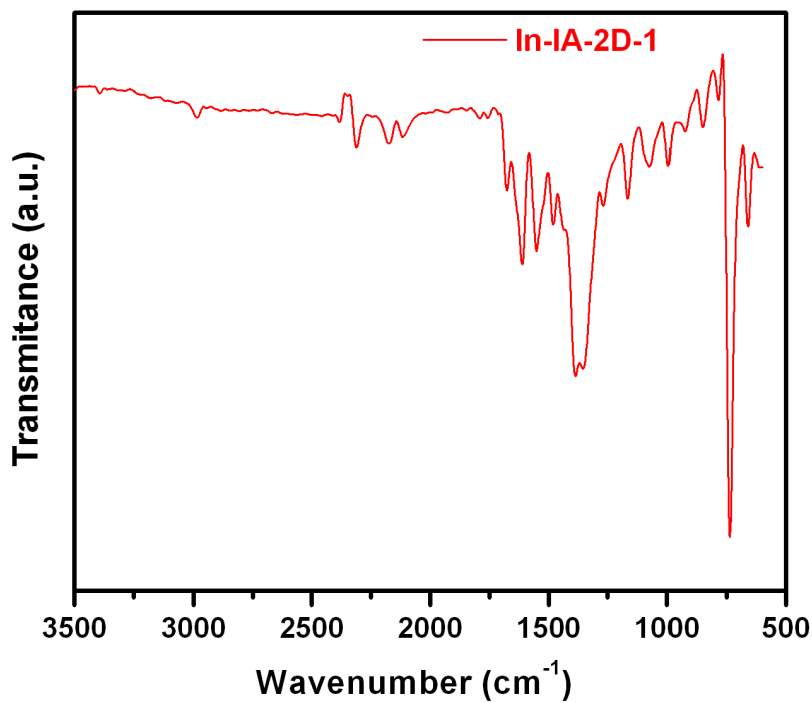


Figure S3. IR spectra of In-IA-2D-1 MOF

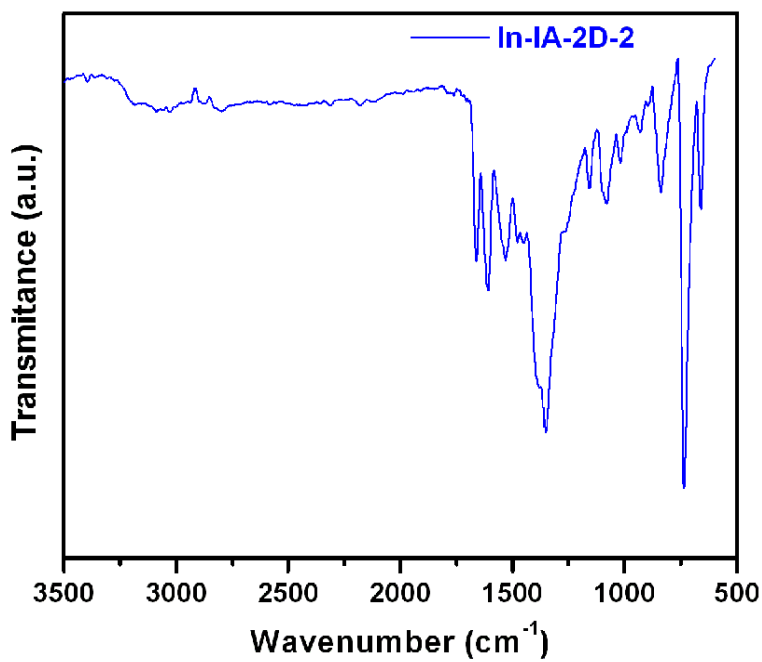


Figure S4. IR spectra of In-IA-2D-2 MOF

Section S2. Single crystal X-ray diffraction data collection, structure solution and refinement procedures:

General data collection and refinement procedures:

Data was collected on a Super Nova Dual source X-ray Diffractometer system (Agilent Technologies) equipped with a CCD area detector and operated at 250 W (50 kV, 0.8 mA) to generate Mo K α radiation ($\lambda = 0.71073 \text{ \AA}$) and Cu K α radiation ($\lambda = 1.54178 \text{ \AA}$). The crystal reported in this paper was mounted on Nylon CryoLoops (Hampton Research) with Paraton-N (Hampton Research).

Initial scans of each specimen were performed to obtain preliminary unit cell parameters and to assess the mosaicity (breadth of spots between frames) of the crystal to select the required frame width for data collection. CrysAlis^{Pro} program software suite to carry out was used overlapping ϕ and ω scans at detector (2θ) settings ($2\theta = 28$). Following data collection, reflections were sampled from all regions of the Ewald sphere to redetermine unit cell parameters for data integration. In no data collection was evidence for crystal decay encountered. Following exhaustive review of collected frames the resolution of the dataset was judged. Data were integrated using CrysAlis^{Pro} software with a narrow frame algorithm. Data were subsequently corrected for absorption by the program SCALE3 ABSPACK¹ scaling algorithm.

These structures were solved by direct method and refined using the SHELXTL 97² software suite. Atoms were located from iterative examination of difference F-maps following least squares refinements of the earlier models. Final model was refined anisotropically (if the number of data permitted) until full convergence was achieved. Hydrogen atoms were placed in calculated positions (C-H = 0.93 \AA) and included as riding atoms with isotropic displacement parameters 1.2-1.5 times U_{eq} of the attached C atoms. Data were collected at 100(2) K for the MOF presented in this paper. This lower temperature was considered to be optimal for obtaining the best data. The structure was examined using the Addsym subroutine of PLATON³ to assure that no additional symmetry could be applied to the models. The ellipsoids in ORTEP diagrams are displayed at the 50% probability level unless noted otherwise. For all structures we note that elevated R-values are commonly encountered in MOF crystallography for the reasons expressed above by us and by other research groups.⁴⁻¹³ Crystallographic data (excluding

structure factors) for the structures are reported in this paper have been deposited in CCDC as deposition No. CCDC 894117-894118. Copies of the data can be obtained, free of charge, on application to the CCDC, 12 Union Road, Cambridge CB2 1EZ, U.K. [fax: þ 44 (1223) 336 033; e-mail: deposit@ccdc.cam.ac.uk].

1. CrysAlisPro, Version 1.171.33.66; Oxford Diffraction Ltd.: Abingdon, U.K., 2010.
2. G. M. Sheldrick, (1997). SHELXS '97 and SHELXL '97. University of Göttingen, Germany.
3. A. L. Spek (2005) PLATON, A Multipurpose Crystallographic Tool, Utrecht University, Utrecht, The Netherlands.
4. L. A. Dakin, P. C. Ong, J. S. Panek, R. J. Staples, and P. Stavropoulos, *Organometallics*, 2000, **19**, 2896.
5. S. Noro, R. Kitaura, M. Kondo, S. Kitagawa, T. Ishii, H. Matsuzaka, and M. Yamashita, *J. Am. Chem. Soc.* 2002, **124**, 2568.
6. M. Eddaoudi, J. Kim, D. Vodak, A. Sudik, J. Wachter, M. O'Keeffe, and O. M. Yaghi, *Proc. Natl. Acad. Sci. USA*, 2002, **99**, 4900.
7. R. A. Heintz, H. Zhao, X. Ouyang, G. Grandinetti, J. Cowen, and K. R. Dunbar, *Inorg. Chem.* 1999, **38**, 144.
8. K. Biradha, Y. Hongo, and M. Fujita, *Angew. Chem. Int. Ed.* 2000, **39**, 3843.
9. P. Grosshans, A. Jouaiti, M. W. Hosseini, and N. Kyritsakas, *New J. Chem, (Nouv. J. Chim.)* 2003, **27**, 793.
10. N. Takeda, K. Umemoto, K. Yamaguchi, and M. Fujita, *Nature (London)* 1999, **398**, 794.
11. M. Eddaoudi, J. Kim, N. Rosi, D. Vodak, J. Wachter, M. O'Keeffe, and O. M. Yaghi, *Science*, 2002, **295**, 469.
12. B. Kesanli, Y. Cui, M. R. Smith, E. W. Bittner, B. C. Bockrath, and W. Lin, *Angew. Chem. Int. Ed.* 2005, **44**, 72.
13. F. A. Cotton, C. Lin, and C. A. Murillo, *Inorg. Chem.* 2001, **40**, 478.

In-IA-2D-1 (Orthorhombic)

Experimental and refinement details for In-IA-2D-1:

A colorless plate like crystal ($0.35 \times 0.28 \times 0.16 \text{ mm}^3$) of **In-IA-2D-1** was placed in 0.7 mm diameter nylon CryoLoops (Hampton Research) with Paraton-N (Hampton Research). The loop was mounted on a Super Nova Dual source X-ray Diffractometer system (Agilent Technologies) equipped with a CCD area detector and operated at 250 W power (50 kV, 0.8 mA) to generate Mo K α radiation ($\lambda = 0.71073 \text{ \AA}$) at 100(2) K in a liquid N₂ cooled stream of nitrogen. A total of 15548 reflections were collected of which 7034 were unique. The range of θ was from 3.29 to 29.15. Analysis of the data showed negligible decay during collection. The structure was solved in the orthorhombic $Pna2_1$ space group, with $Z = 4$, using direct methods. All non-hydrogen atoms were refined anisotropically with hydrogen atoms generated as spheres riding the coordinates of their parent atoms. We have repeatedly collected the single crystal XRD data of In-IA-2D-1 at different temperature (90, 120, 150K). We would like to mention that each time during the refinement of crystal structure we encountered two electron densities within the framework cavity apart from dimethyl ammonium cation. However, assigning these electron densities with isolated O atoms, leads to highly distorted O atoms, although the refinement become stable with decreased R factor and goodness of fit. Hence, we believe that two water molecules reside inside the asymmetric unit of In-IA-2D-1, however, the O atoms of water molecules have very high thermal parameters apart from In-IA and (CH₃)₂NH₂ cations with several IUCr checkcif errors. Hence we have decided to use the SQUEEZE routine to remove these unstable and highly distorted water molecules from the pores of In-IA-2D-1. It should be noted that SQUEEZE structure is very stable with minimal IUCr checkcif problems, less R factor and goodness of fit. In this manuscript we have provided the SQUEEZE applied cif file of In-IA-2D-1. Final full matrix least-squares refinement on F^2 converged to $R_1 = 0.0725 (F > 2\sigma F)$ and $wR_2 = 0.2213$ (all data) with GOF = 1.132. CCDC 894117

Refine_special_details:

We believe this distortion in the benzene ring in In-IA-2D-1 structure appears due to possible merohedral or pseudo-merohedral twinning not due to a static or dynamic disorder. As a result despite lowering the data collection temperature to 110 K this distortion remains persistent. A close look of the .res file will show that the structure contains a twinning with a BASF parameter 0.545. This indicates a 50/50 twinning in the crystal lattice. In order to overcome this distortion we have used 8 EADP and 3 FLAT commands in the .res file. These EADP and FLAT commands are listed herein.

```
EADP O1 O2
EADP O5 O6
EADP C2 C10
EADP C14 C4
EADP C13 C5
EADP C12 C3
EADP C11 C7
EADP C18 C17
FLAT C11 C12 C13 C14
FLAT C13 C14 C15 C16
FLAT C10 C11 C9 C15
```

_Platon_squeeze_details:

The asymmetric unit of In-IA-2D-1 consist two highly distorted water molecules in the pore. we have decided to use the SQUEEZE routine to remove these water molecules from the pores of In-IA-2D-1. We would like to mention that 6.85% amount of disordered solvents (water molecules) were removed from the asymmetric unit of In-IA-2D-1 by the SQUEEZE process.

```
loop_
  _platon_squeeze_void_nr
  _platon_squeeze_void_average_x
  _platon_squeeze_void_average_y
  _platon_squeeze_void_average_z
  _platon_squeeze_void_volume
  _platon_squeeze_void_count_electrons
  _platon_squeeze_void_content
  1 -0.029 0.858 -0.031 764 77 ''
```

Table S1: Crystal data and structure refinement for In-IA-2D-1 (SQUEEZE):

Empirical formula	C ₁₆ H ₈ InO ₈ ,C ₂ H ₈ N
Formula weight	489.14
Temperature	100(2) K
Wavelength	0.71073
Crystal system	Orthorhombic
Space group	<i>Pna2</i> ₁
Unit cell dimensions	$a = 15.8408(4) \text{ \AA}$ $\alpha = 90^\circ$ $b = 16.5349(3) \text{ \AA}$ $\beta = 90^\circ$ $c = 9.94883(14) \text{ \AA}$ $\gamma = 90^\circ$
Volume	2605.86(8)
Z	4
Density (calculated)	1.247
Absorption coefficient	0.940
F(000)	976
Crystal size	0.32 × 0.24 × 0.15 mm ³
Theta range for data collection	3.29– 29.15
Index ranges	-21= h <= 21, -22<= k <= 22, -13<= l <= 13
Reflections collected	15548
Independent reflections	5885
Completeness to theta = 26.02°	99.7 %
Absorption correction	Semi-empirical from equivalents
Refinement method	Full-matrix least-squares on F ²
Data / restraints / parameters	5885/4/208
Goodness-of-fit on F²	1.132
Final R indices [I>2sigma(I)]	R ₁ = 0.0725, wR ₂ = 0.2213
R indices (all data)	R ₁ = 0.820, wR ₂ = 0.2361
Largest diff. peak and hole	2.211 and -1.192 eÅ ⁻³
Flack parameter	0.55 (7)

Crystal data and structure refinement for In-IA-2D-1 (Non SQUEEZE):

Empirical formula	C ₁₆ H ₈ InO ₈ ,C ₂ H ₈ N, (H ₂ O) ₂
Formula weight	525.15
Temperature	100(2) K
Wavelength	0.71073
Crystal system	Orthorhombic
Space group	<i>Pna2</i> ₁
Unit cell dimensions	$a = 15.8408(4) \text{ \AA}$ $\alpha = 90^\circ$ $b = 16.5349(3) \text{ \AA}$ $\beta = 90^\circ$ $c = 9.94883(14) \text{ \AA}$ $\gamma = 90^\circ$
Volume	2605.86(8)
Z	4
Density (calculated)	1.328
Absorption coefficient	0.95
F(000)	1040
Crystal size	0.32 × 0.24 × 0.15 mm ³
Theta range for data collection	3.29– 29.15
Index ranges	-21= h <= 21, -22<= k <= 22, -13<= l <= 13
Reflections collected	15548
Independent reflections	5885
Completeness to theta = 26.02°	99.7 %
Absorption correction	Semi-empirical from equivalents
Refinement method	Full-matrix least-squares on F ²
Data / restraints / parameters	5885/4/208
Goodness-of-fit on F²	1.060
Final R indices [I>2sigma(I)]	R ₁ = 0.0768, wR ₂ = 0.2230
R indices (all data)	R ₁ = 0.896, wR ₂ = 0.2439
Largest diff. peak and hole	1.823 and -1.280 eÅ ⁻³
Flack parameter	0.56 (9)

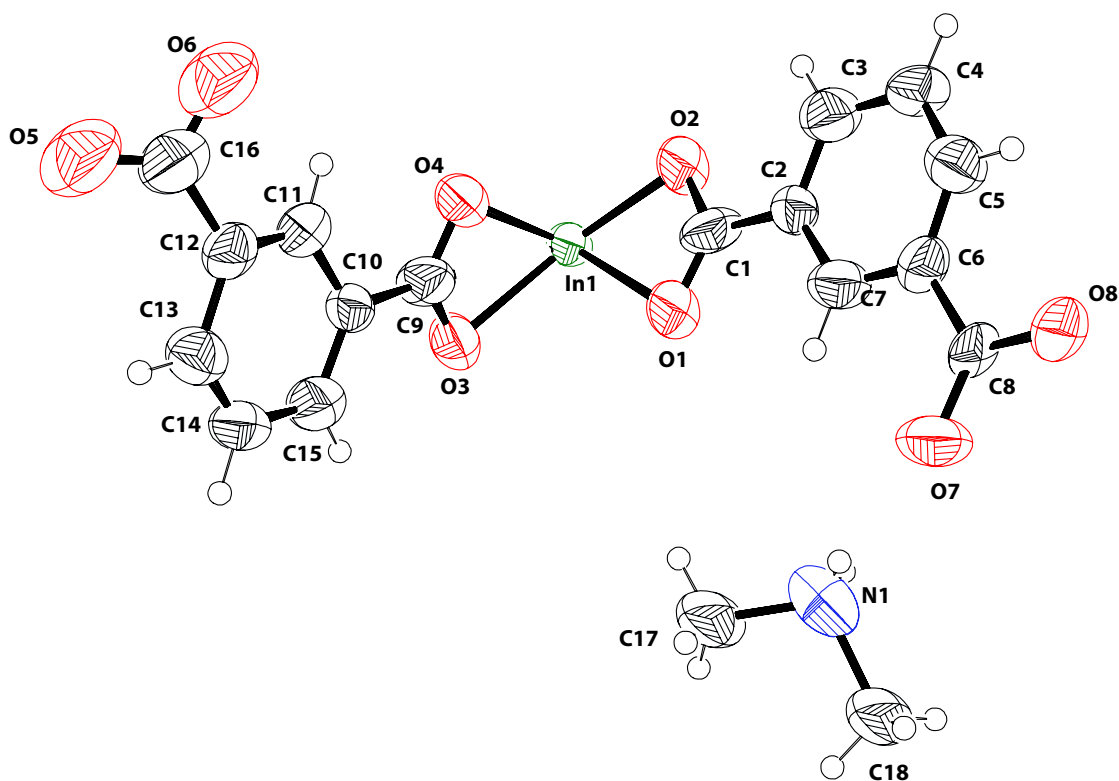


Figure S5. ORTEP diagram (50% probability) of the asymmetric unit of In-IA-2D-1.

In-IA-2D-2 (Monoclinic)

Experimental and refinement details for In-IA-2D-2:

A colorless block like crystal ($0.35 \times 0.27 \times 0.15 \text{ mm}^3$) of **In-IA-2D-2** was placed in 0.7 mm diameter nylon CryoLoops (Hampton Research) with Paraton-N (Hampton Research). The loop was mounted on a Super Nova Dual source X-ray Diffractometer system (Agilent Technologies) equipped with a CCD area detector and operated at 250 W power (50 kV, 0.8 mA) to generate Cu K α radiation ($\lambda = 1.54178 \text{ \AA}$) at 100(2) K in a liquid N₂ cooled stream of nitrogen. A total of 8741 reflections were collected of which 4027 were unique. The range of θ was from 4.50 to 70.72. Analysis of the data showed negligible decay during collection. The structure was solved in the Monoclinic $P2_1/c$ space group, with $Z = 4$, using direct methods. All non-hydrogen atoms were refined anisotropically with hydrogen atoms generated as spheres riding the coordinates of their parent atoms. Final full matrix least-squares refinement on F^2 converged to $R_1 = 0.0684$ ($F > 2\sigma F$) and $wR_2 = 0.1826$ (all data) with GOF = 0.993. CCDC 894118

Refine_special_details:

the solvent DMF molecule has been refined as isotropic due to large anisotropic displacement of N atom of DMF molecule even after several refinements.

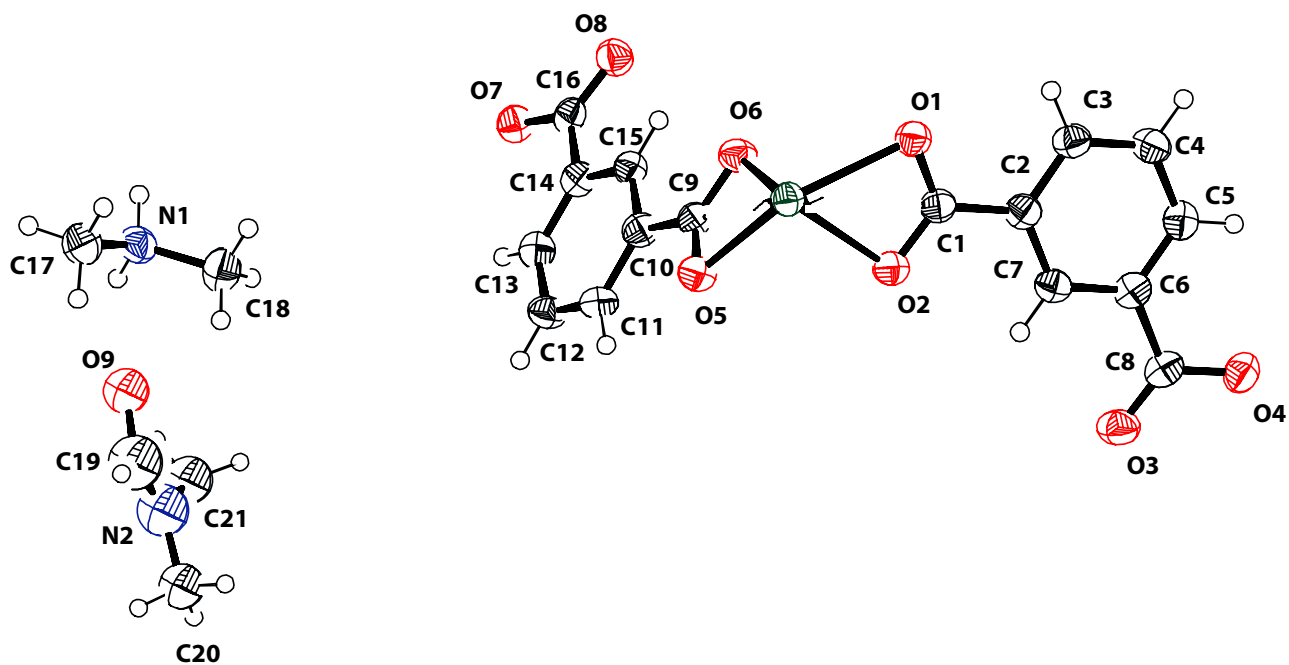


Figure S6. ORTEP diagram (50% probability) of the asymmetric unit of In-IA-2D-2 MOF.

Table S2: Crystal data and structure refinement for In-IA-2D-2:

Empirical formula	$C_{16}H_8InO_8, C_3H_7NO, C_2H_8N$
Formula weight	562.23
Temperature	100(2) K
Wavelength	1.54178 Å
Crystal system	Monoclinic
Space group	$P2_1/c$
Unit cell dimensions	$a = 11.9876(3) \text{ \AA} \quad \alpha = 90^\circ$ $b = 13.0329(4) \text{ \AA} \quad \beta = 125.260(2)^\circ$ $c = 18.3012(6) \text{ \AA} \quad \gamma = 90^\circ$
Volume	2334.70(12)
Z	4
Density (calculated)	1.600
Absorption coefficient	8.564
F(000)	1136
Crystal size	$0.35 \times 0.27 \times 0.15 \text{ mm}^3$
Theta range for data collection	4.50 – 70.72
Index ranges	$-14 \leq h \leq 8, -15 \leq k \leq 15, -17 \leq l \leq 22$
Reflections collected	8741
Independent reflections	4027
Completeness to theta	96.0 %
Absorption correction	Semi-empirical from equivalents
Refinement method	Full-matrix least-squares on F^2
Data / restraints / parameters	4486 / 0 / 279
Goodness-of-fit on F^2	0.993
Final R indices [$I > 2\sigma(I)$]	$R_1 = 0.0684, wR_2 = 0.1826$
R indices (all data)	$R_1 = 0.0710, wR_2 = 0.1854$
Largest diff. peak and hole	0.409 and -0.115 e\AA^{-3}

Variable temperature single crystal X-ray (VTSCXRD) of In-IA-2D-2

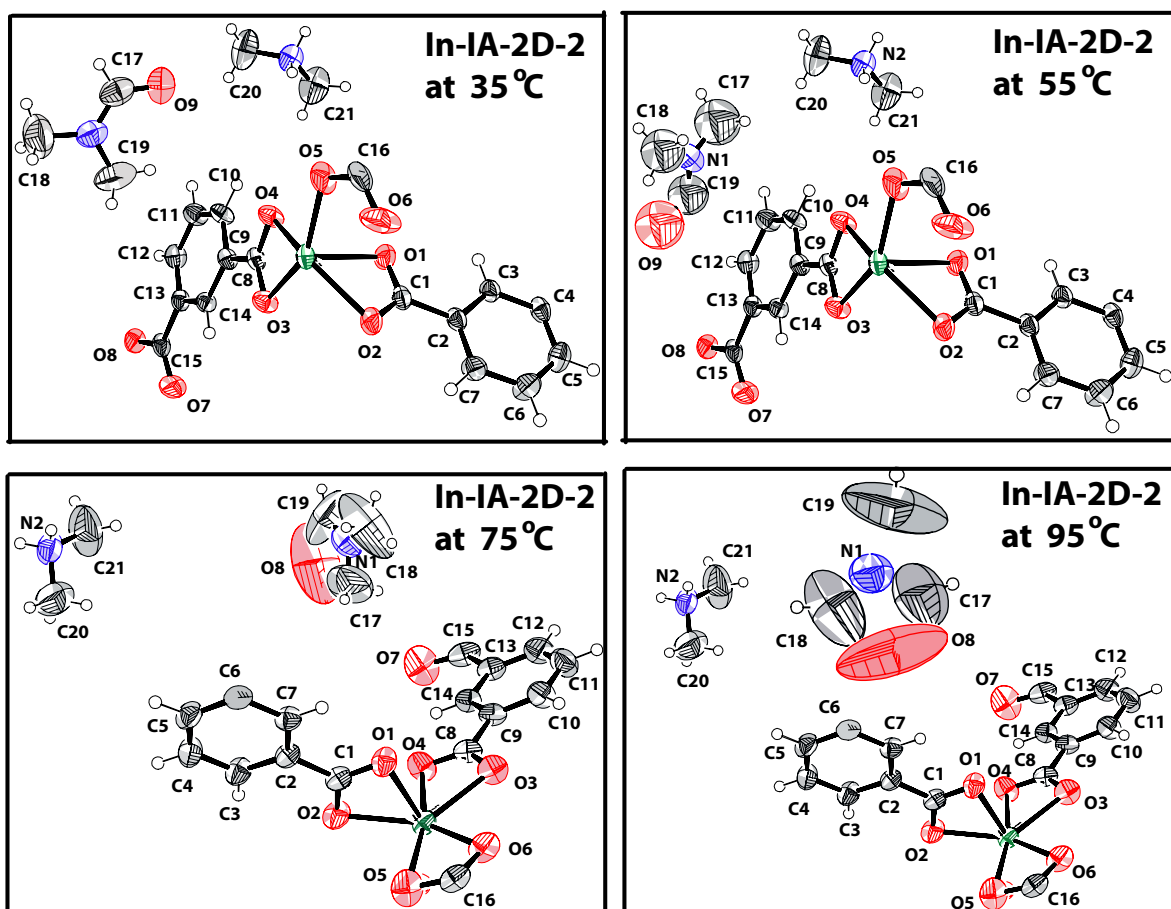


Figure S7. ORTEP diagrams (50% probability) of In-IA-2D-2 single crystal X-ray data at variable temperature (35, 55, 75 and 95 °C).

Section S3. TGA data and the thermal stability of MOFs:

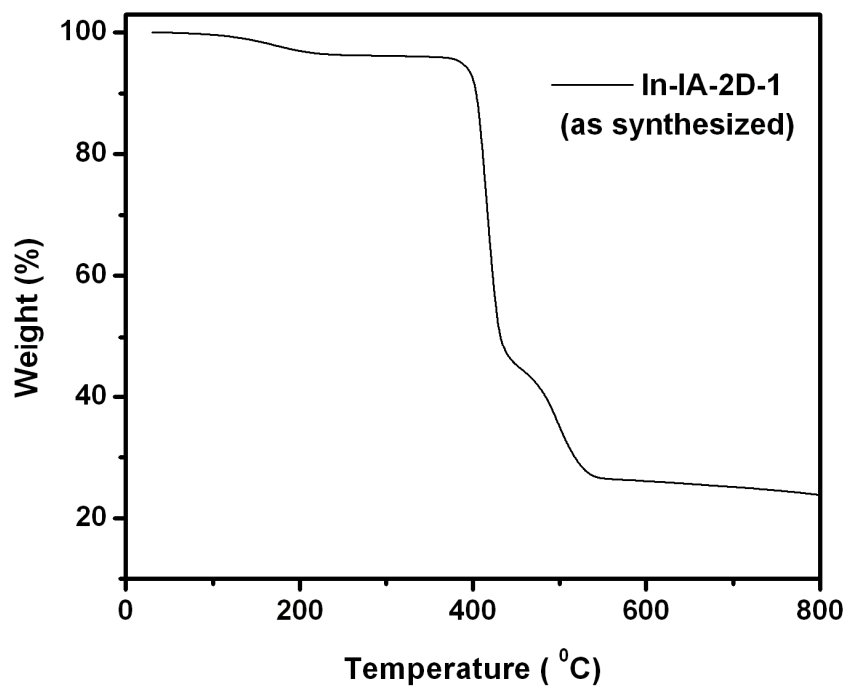


Figure S8. Thermo gravimetric analysis (TGA) data of In-IA-2D-1.

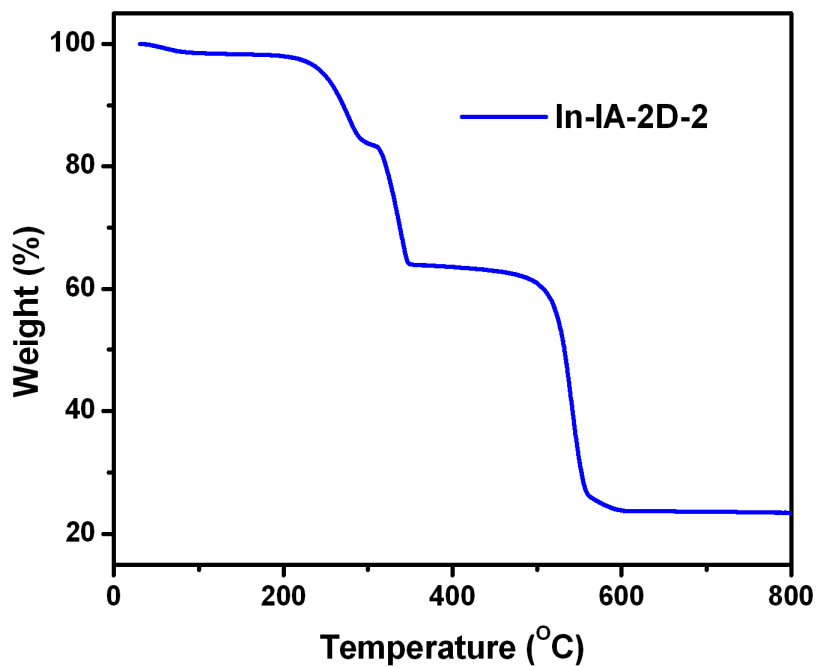


Figure S9. Thermo gravimetric analysis (TGA) data of In-IA-2D-2.

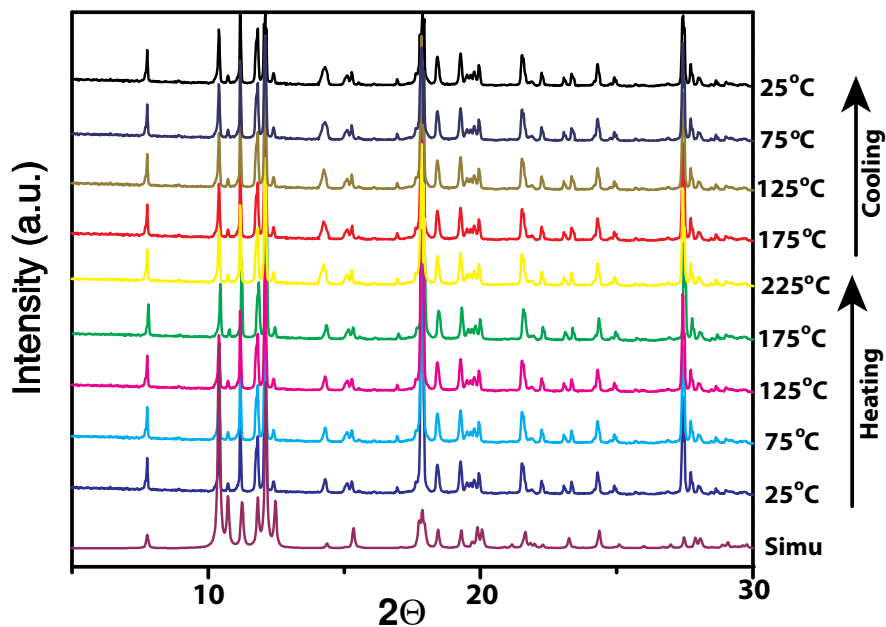


Figure S10. Variable temperature powder X-ray diffraction VTPXRD data of In-IA-2D-1 comparison with the simulated one clearly indicates its high crystallinity as well as thermal stability at broad temperature range (25 °C to 225 °C).

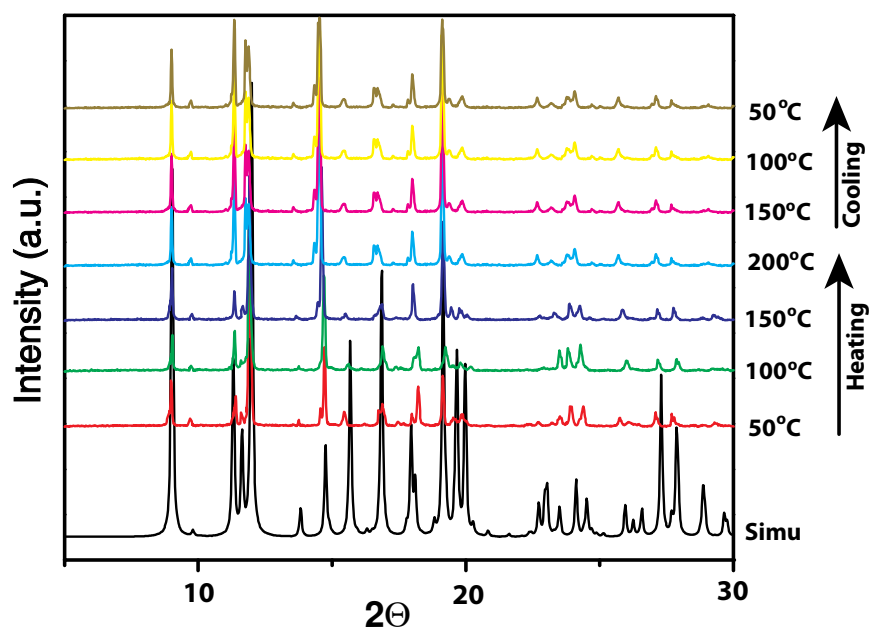


Figure S11. Variable temperature powder X-ray diffraction VTPXRD data of In-IA-2D-2 comparison with the simulated one clearly indicates its high crystallinity as well as thermal stability at broad temperature range (50 °C to 200 °C).

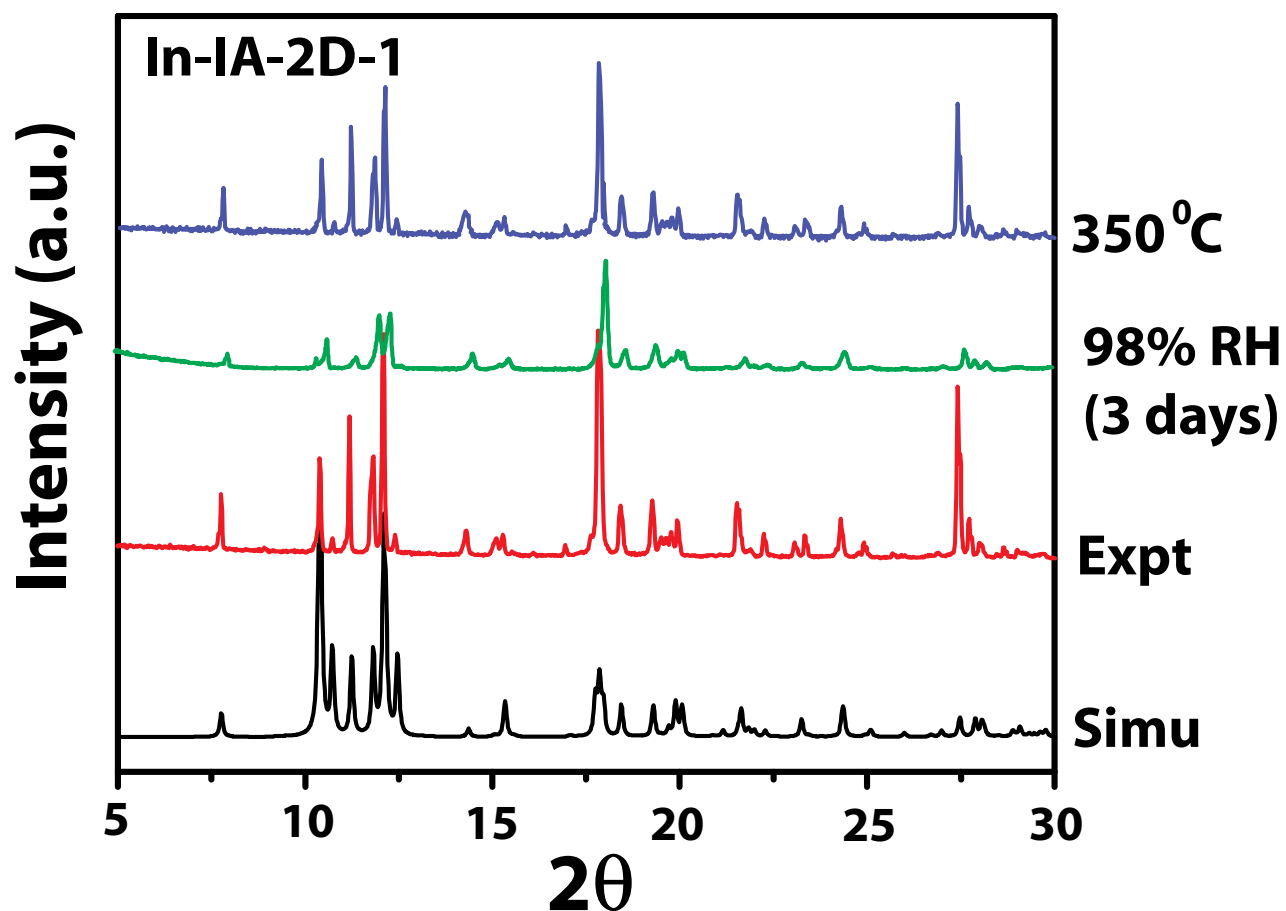


Figure S12. Powder X-ray diffraction analysis of as synthesized (Expt), humidified (under 98% RH for 3 days) and preheated at 350 °C of In-Ia-2D-1 in comparison with the simulated one clearly indicates its high crystallinity, purity as well as stability at long time humidified condition.

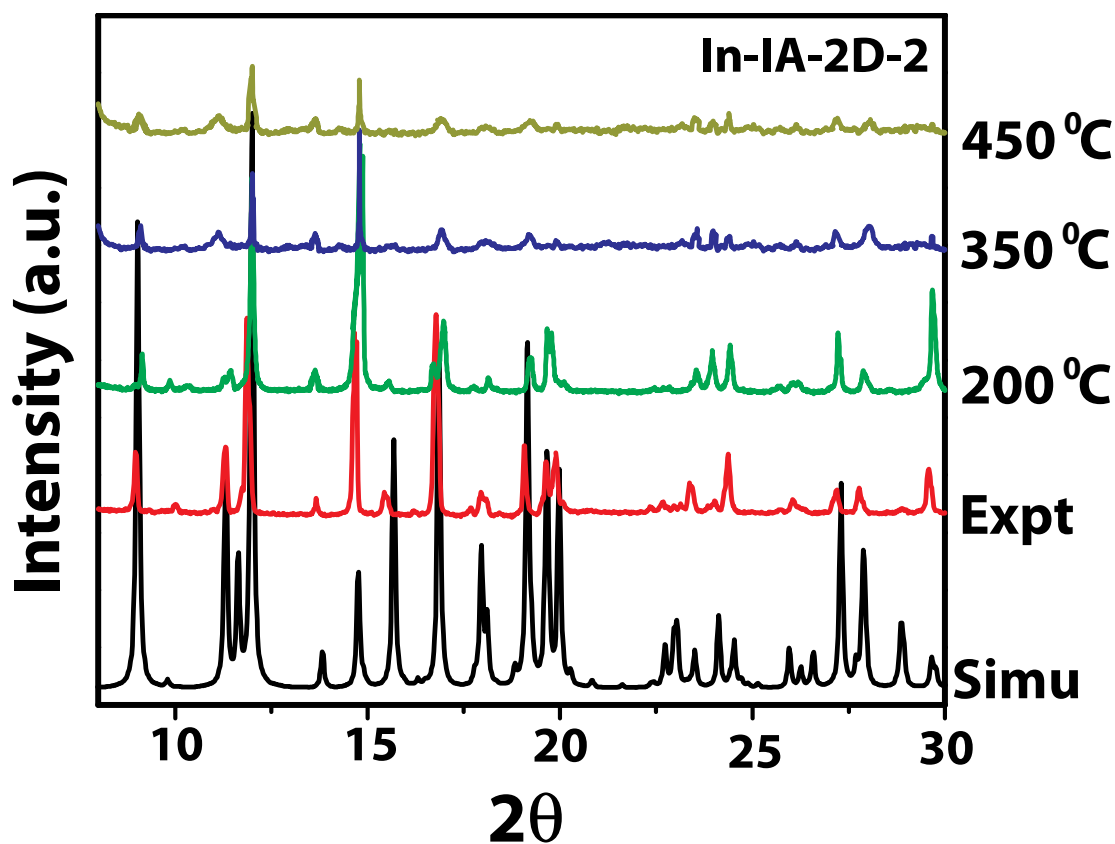


Figure S13. Powder X-ray diffraction analysis of as synthesized (Expt) and pre heated (200 °C and 350 °C) samples of In-IA-2D-2 in comparison with the simulated one which clearly indicates its high crystallinity and stability at higher temperatures.

We took three batches of In-IA-2D-2 samples and separately heated 200 °C, 350 °C and 450 °C in a furnace for 2 hours followed by cooling up to room temperature. PXRD pattern of these three samples indicates its crystallinity and framework stability at higher temperature.

We have performed the elemental analysis (CHN) of preheated (350 °C) In-IA-2D-2 samples, Found: C (44.08%), H (1.85%), N (0.01%). The % of N is ~0 signifies that, absence of N atom in preheated (350 °C) In-IA-2D-2 sample which eventually matches with the molecular formula of $\{In (IA)_2 H^+\}$ [Calc: C (43.35%), H (1.89%), N (0%)]

We have also performed proton conductivity of preheated (350 °C) In-IA-2D-2 under 98% RH. It is interesting to note that, this material does not show any conductivity due to absence of carrier dimethylammonium cation inside the framework.

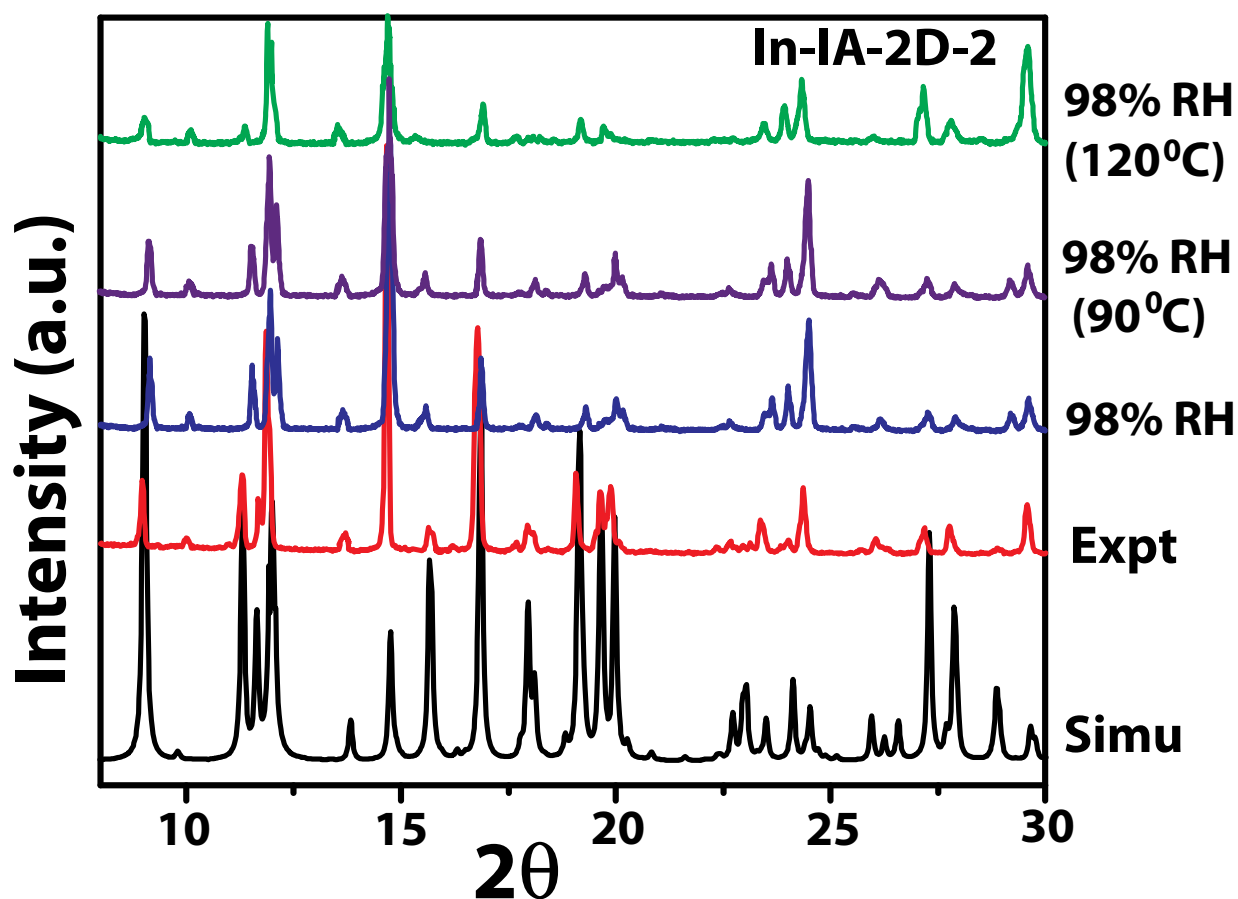


Figure S14. Powder X-ray diffraction (PXRD) data of In-IA-2D-2 as synthesized (Expt), 98% Relative humidified condition, 98% RH then heated to 90 °C and 120 °C of In-Ia 2D-2, strongly indicate its high crystallinity and stability under Humidified condition.

In order to confirm the stability and purity of In-IA-2D-2 under 98% RH for longer period, we kept the sample under humidification inside the humidified chamber for 72 hrs (3 days) and then measured the PXRD experiment. It is interesting to note that after humidification the PXRD pattern of In-IA-2D-2 is matching with the simulated one. We have also heated this humidified In-IA-2D-2 (3 days under 98% RH) to 90 °C and 120 °C for 1 days then measured PXRD. The PXRD pattern are also matching with the simulated one. Thus it signifies the bulk purity and framework stability remains intact after humidification as well as humidification followed by heating.

Section S4. Single crystal structures of MOFs:

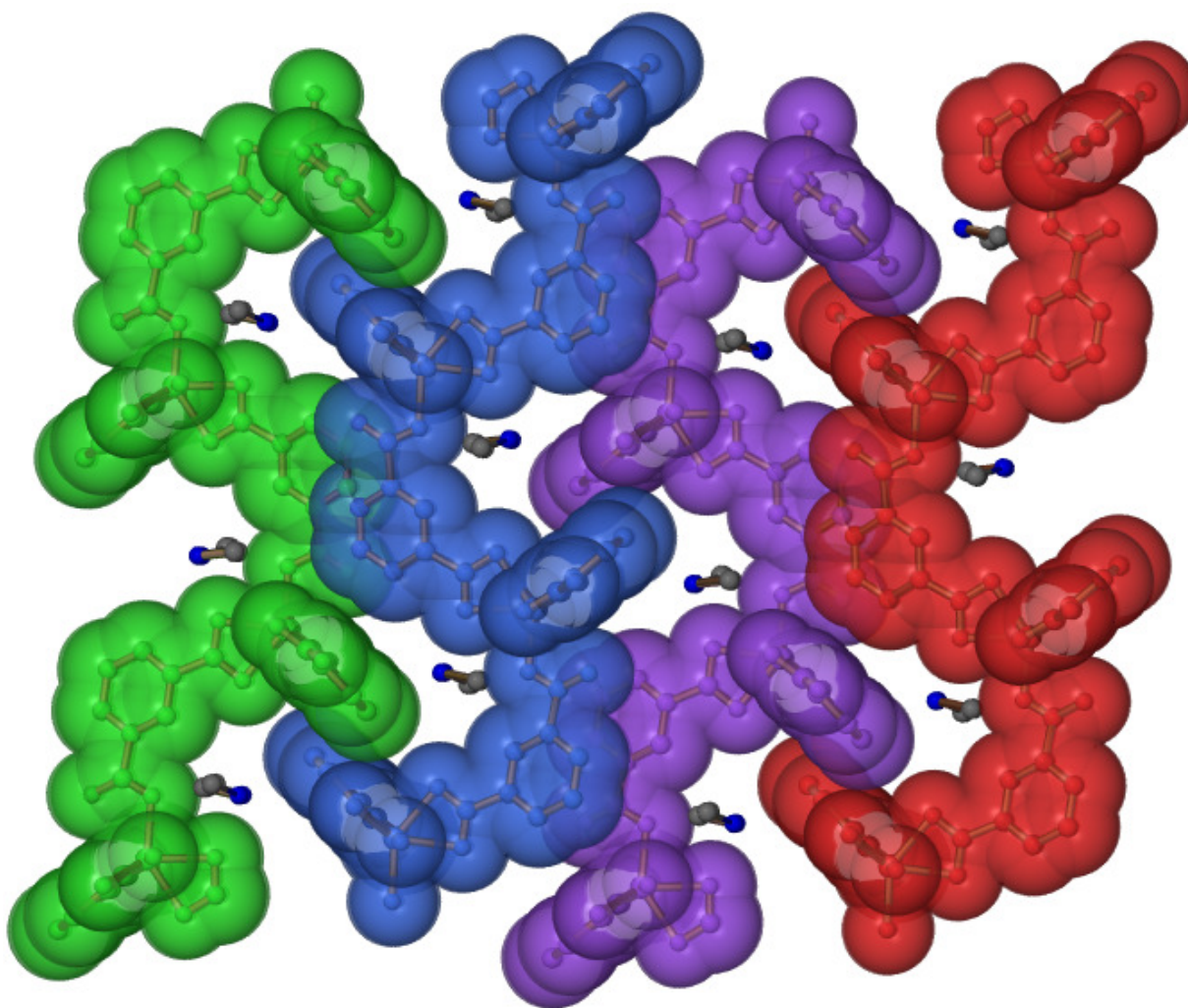


Figure S15. Crystal structure of In-IA-2D-1 shows dimethylammonium cations are resides inside the void space between two dimensional layers. Open space inside the two dimensional layers facilitate the proton hopping in humid conditions (98% RH).

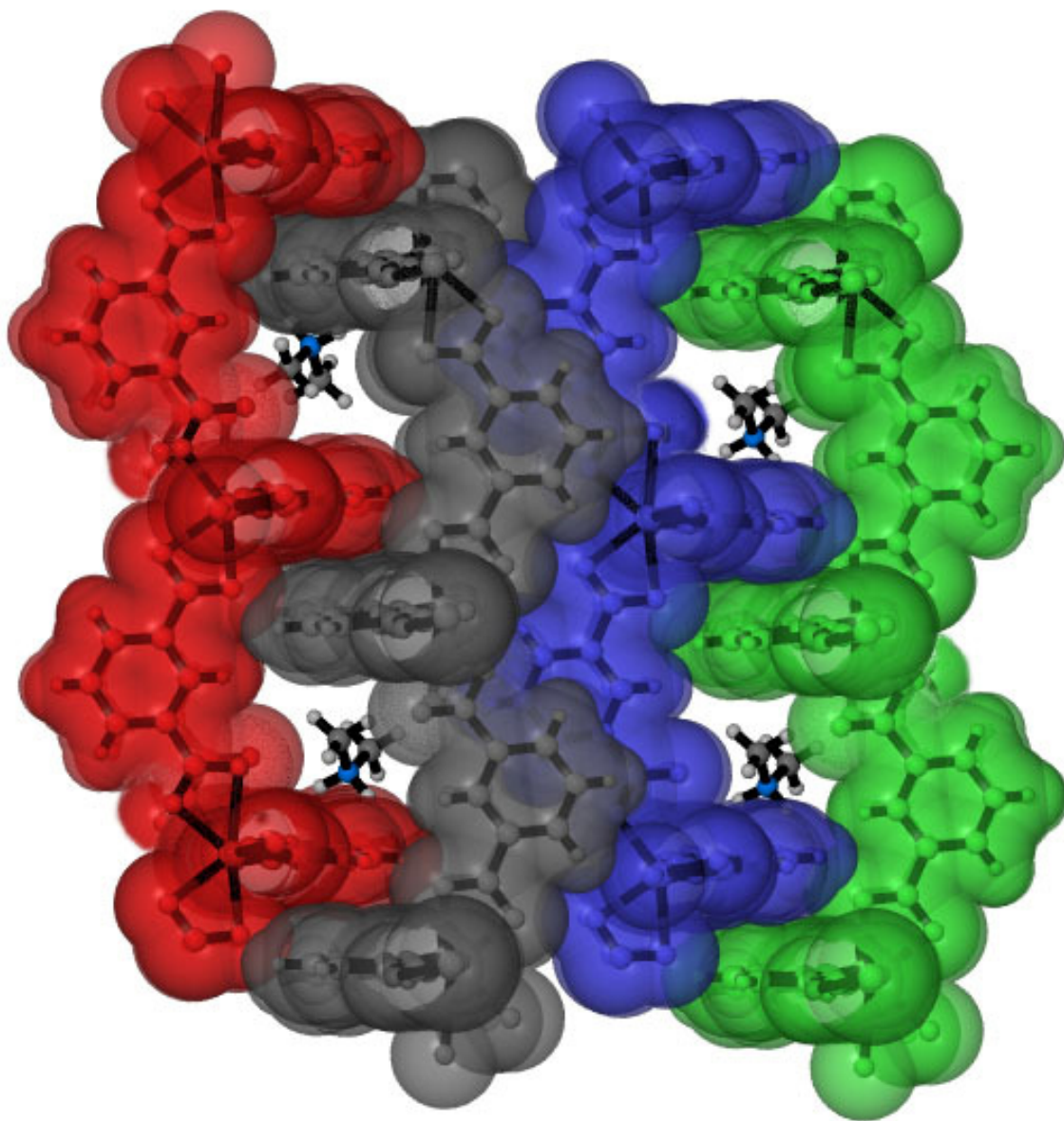


Figure S16. Crystal structure of In-IA-2D-2 shows dimethylammonium cations are resides inside the void space between these two dimensional layers. (For clarity DMF has been removed from the crystal structure)

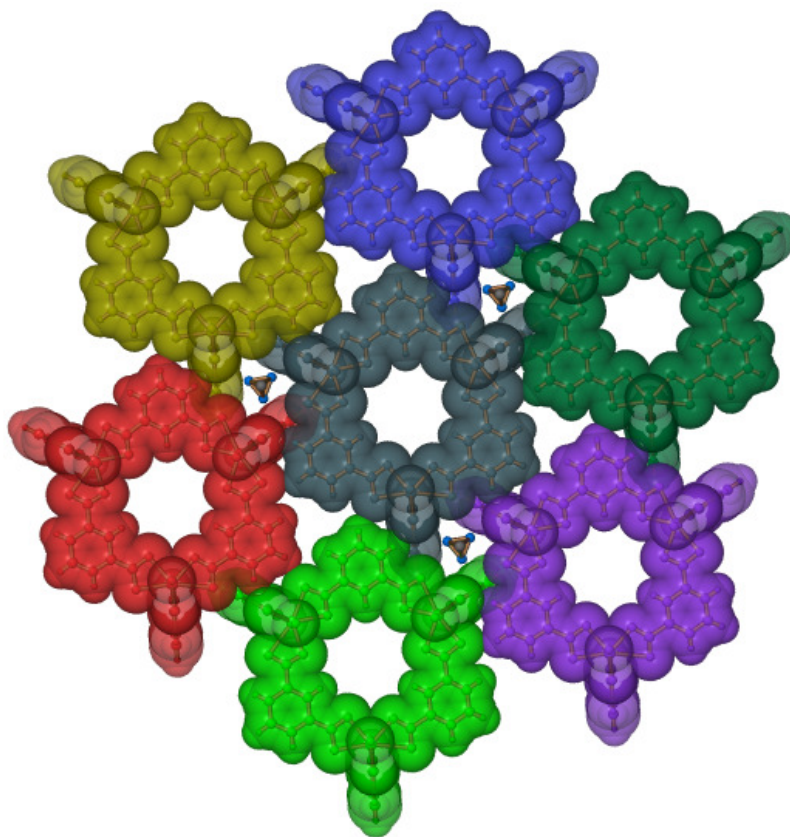


Figure S17. Crystal structure of reported In-IA-1D shows dimethylammonium cations occupies adjacent to the void space between this nanotubular architecture.

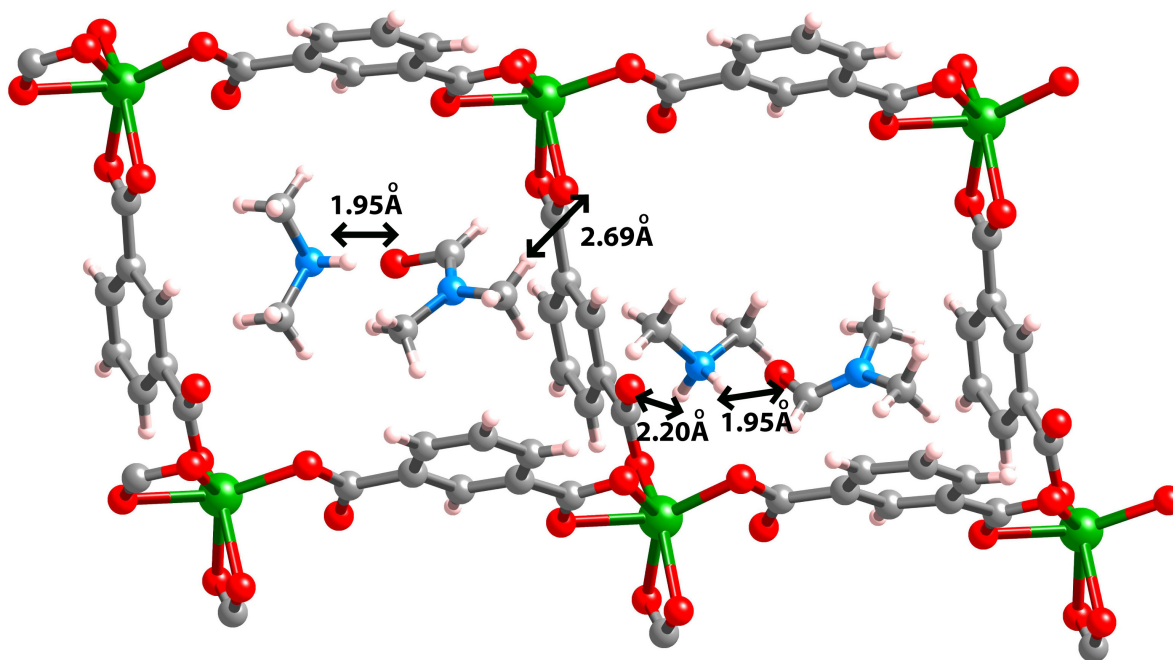


Figure S18. Intermolecular distance between proton hopping sites in the crystal structure of In-IA-2D-2.

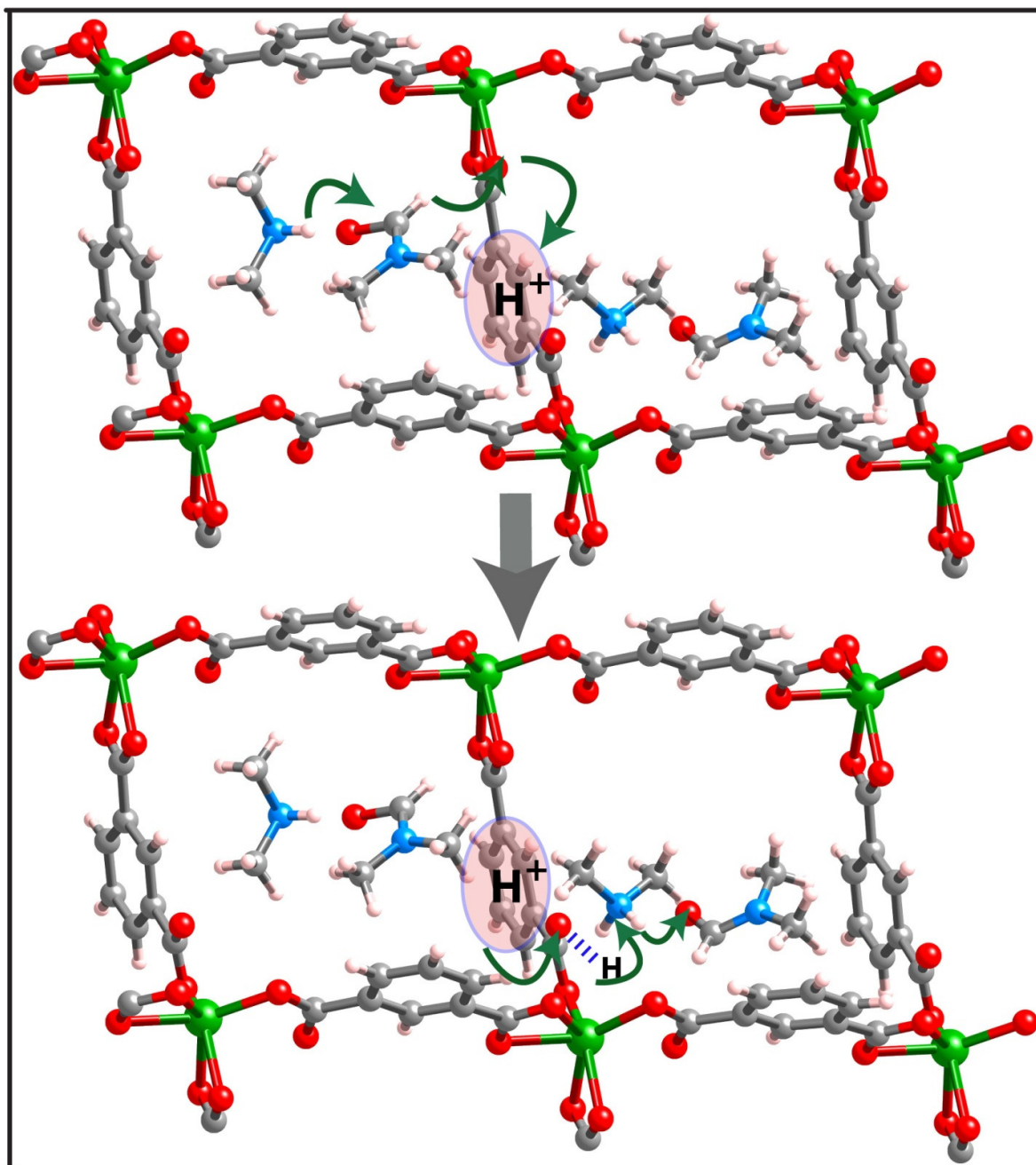


Figure S19. Schematic representation and possible proton hopping mechanism of In-IA-2D-2 MOF under anhydrous condition. The arrows indicate the possible movement of the H^+ ion.

Section S5. Water vapor adsorption studies of In-IA-2D-1 and -2 MOFs:

110 mg of as synthesised In-IA-2D-1 has been taken and dried at room temperature upto 4 hours. Water vapor uptake capability of In-IA-2D-1 are 2.9 wt% at STP .

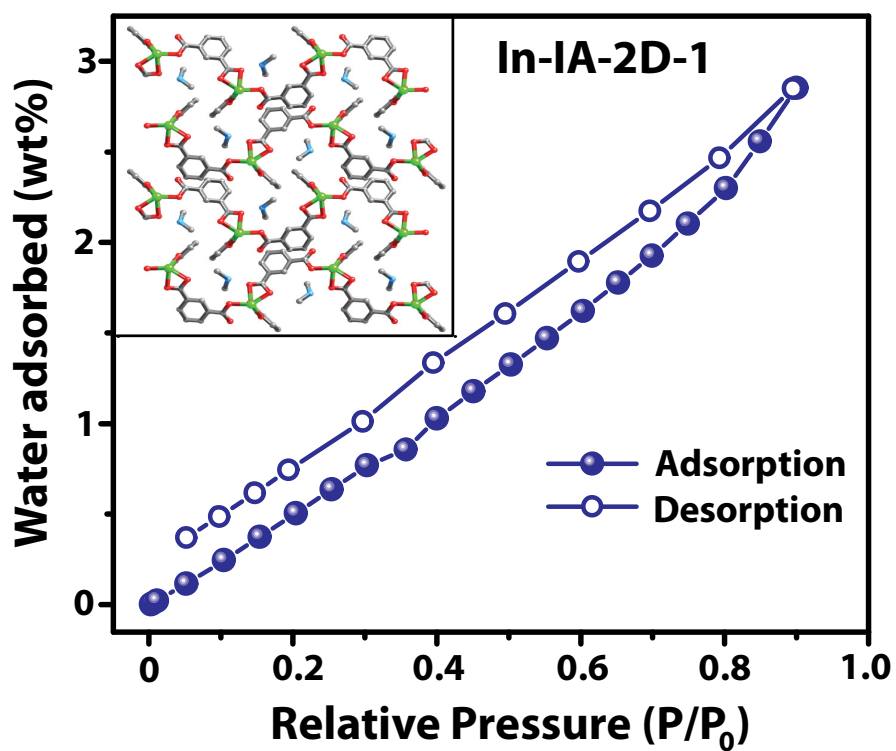


Figure S20. Water vapor adsorption plot of In-IA-2D-1 at STP, which shows 2.9 wt% water vapor adsorbed by In-IA-2D-1 at STP.

In-IA-2D-2, 110 mg of as synthesized sample was taken and dried at room temperature upto 4 hrs. These samples were used for water vapor adsorption measurement. In-IA-2D-2 takes up 4.1 wt% water vapor at STP.

Another fresh batch of as synthesized sample of In-IA-2D-2 (110 mg) was heated at 90 °C for 4 hours and then measured water vapor adsorption. Preheated In-IA-2D-2 takes up 7.3 wt% water vapor at STP

The reason behind this high uptake could be the removal of the DMF molecule from In-IA-2D-2 framework at 90 °C under evacuation.

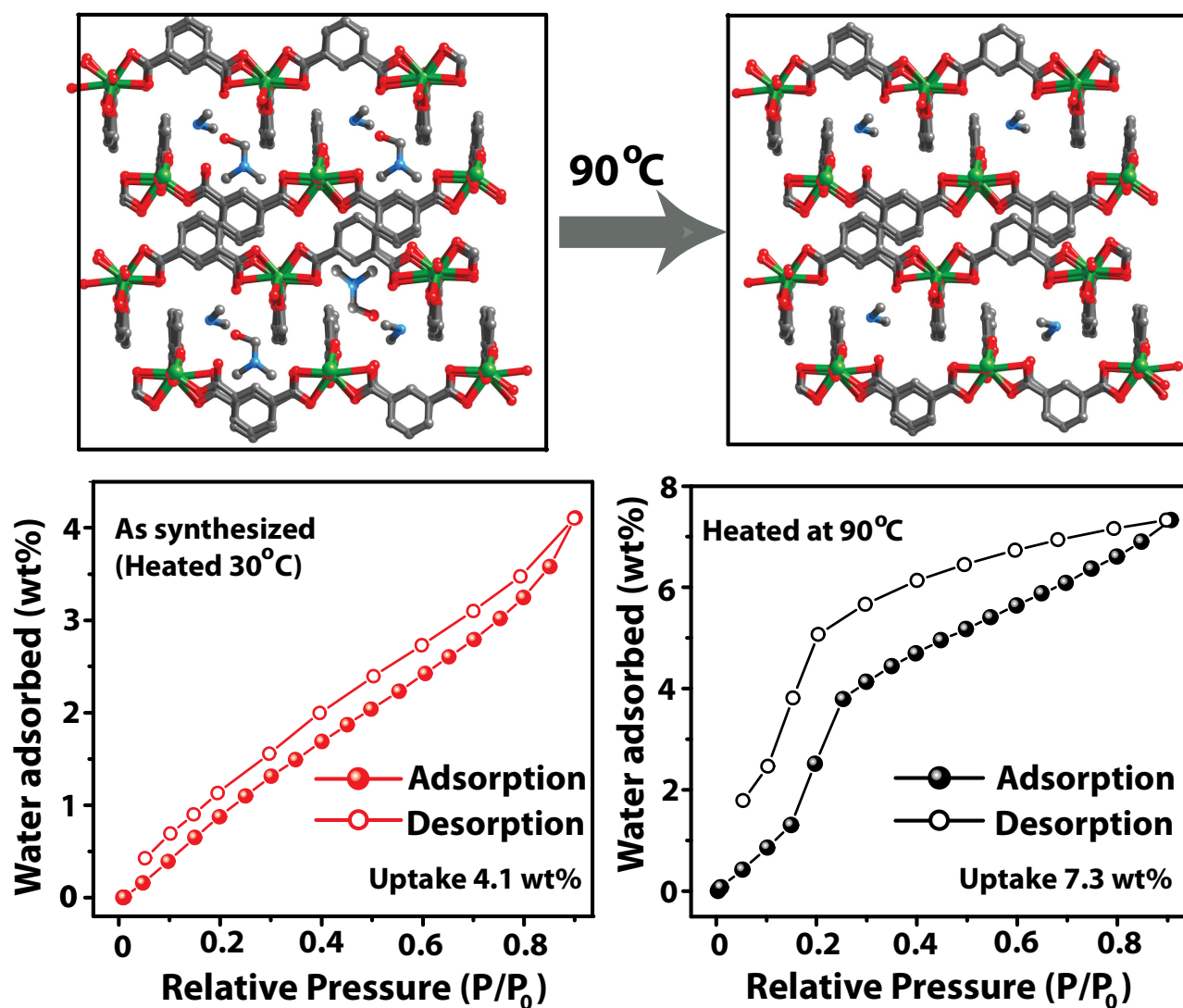


Figure S21. Schematic representation of increasing hydrophilicity of In-IA-2D-2 via DMF removal at 90 °C, confirmed by water vapor adsorption experiment at STP.

Calculation of water content molecular formula at 98% RH of In-IA-2D-1 and In-IA-2D-2:

For In-IA-2D-1,

$$2.85 \text{ wt\% H}_2\text{O uptake} = 2.85 \times \text{MW of In-IA-2D-1} / 100 = 2.85 \times 489.14 / 100 = 13.94 \text{ cc H}_2\text{O}$$

$$\text{Number of water molecules for In-IA-2D-1} = 13.94 / 18 = 0.78$$

Similarly for In-IA-2D-2 ,

$$4.1 \text{ wt\% of H}_2\text{O} = 4.1 \times \text{MW of In-IA-2D-2} / 100 = 4.1 \times 562.23 / 100 = 23.05 \text{ cc H}_2\text{O}$$

$$\text{Hence, number of H}_2\text{O molecule for In-IA-2D-2} = 23.05 / 18 = 1.3$$

We have also calculated the possible chemical formula of both these MOFs at 98% RH. As per our calculations ~1.3 water molecules per asymmetric unit of In-IA-2D-1 and ~0.78 water molecules per asymmetric unit of In-IA-2D-2 are absorbed within the pores. Hence, the molecular formula at 98% RH of these MOFs are $[\text{In}(\text{IA})_2 \{(\text{CH}_3)_2\text{NH}_2\}] \cdot 0.78\text{H}_2\text{O}$ and $[\text{In}(\text{IA})_2 \{(\text{CH}_3)_2\text{NH}_2\}(\text{DMF})] \cdot 1.3\text{H}_2\text{O}$, respectively for In-IA-2D-1 and -2.

Section S6. Proton conductivity studies of In-IA-2D-1 and -2 MOFs:

Proton conductivity methods and plots :

Proton conductivity was measured by a quasi-two-probe method, with a Solartron 1287 Electrochemical Interface with 1255B frequency response analyzer. As synthesized samples of In-IA-2D-1 and -2 were made pellet of 0.6 mm and 1.25 mm thickness, with 6.5 mm diameter under humidified condition for 24 hours and then subject to analysis for proton conduction. The resistances were calculated from the semicircle of the Nyquist plots. The activation energy values were obtained from the slope by least square fitting of the straight line. If the data points are (x_1, y_1) , (x_2, y_2) ,, (x_n, y_n) where x is the independent variable and y is the dependent variable. The fitting curve $f(x)$ has the deviation (error) d from each data point, i.e., $d_1 = y_1 - f(x_1)$, $d_2 = y_2 - f(x_2)$, ..., $d_n = y_n - f(x_n)$. According to the method of least squares, the best fitting curve has the properties:

$$\Pi = d_1^2 + d_2^2 + \dots + d_n^2 = \sum_{i=1}^n d_i^2 = \sum_{i=1}^n [y_i - f(x_i)]^2 = \text{a minimum}$$

N.B. From the semicircle we got the resistance **R** (Ohm). Now, from diameter **r** (mm) and thickness **A** (mm) proton conductivity (σ) value can be calculated by the following equation,

$$\sigma = A / (R \times \pi r^2) \quad \text{Scm}^{-1}$$

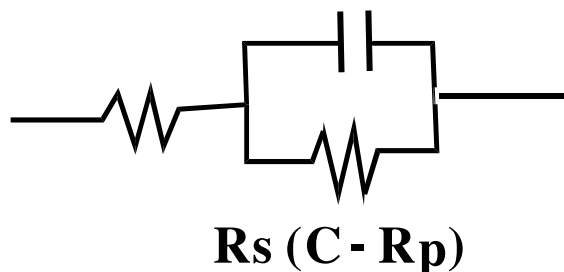


Figure S22 : Equivalent circuit model representation of the Nyquist plot.

For high-temperature proton conductivity measurements, the pellets were inserted within a humidification chamber, which was encircled with a controlled heating coil attached with an automated temperature controller. The heat flow within the temperature controller was controlled by a dimerstat accordingly. The temperature of the chamber was measured by an infrared temperature sensor attachment, having a sensing accuracy of ± 0.5 °C.

For low-temperature proton conductivity measurements, the pellets were inserted within a humidification chamber, which was encircled with a water circulation coil attached with a chiller integrated with an automated temperature controller. The heat flow within the chamber was controlled by the chiller accordingly. The temperature of the chamber was measured by an infrared temperature sensor attachment, having a sensing accuracy of ± 0.5 °C.

Table S3: Low temperature proton conductivity of In-IA-2D-1 and -2 :

Serial no	In-IA-2D-1		In-IA-2D-2	
	Temperature	Proton conductivity value (98% RH)	Temperature	Proton conductivity value (98% RH)
1	5 °C	$5.65 \times 10^{-4} \text{ Scm}^{-1}$	5 °C	$6.19 \times 10^{-5} \text{ Scm}^{-1}$
2	10 °C	$8.22 \times 10^{-4} \text{ Scm}^{-1}$	10 °C	$7.78 \times 10^{-5} \text{ Scm}^{-1}$
3	15 °C	$1.13 \times 10^{-3} \text{ Scm}^{-1}$	15 °C	$1.00 \times 10^{-4} \text{ Scm}^{-1}$
4	20 °C	$1.81 \times 10^{-3} \text{ Scm}^{-1}$	20 °C	$1.56 \times 10^{-4} \text{ Scm}^{-1}$
5	25 °C	$3.01 \times 10^{-3} \text{ Scm}^{-1}$	23 °C	$2.13 \times 10^{-4} \text{ Scm}^{-1}$
6	27 °C	$3.37 \times 10^{-3} \text{ Scm}^{-1}$	27 °C	$4.20 \times 10^{-4} \text{ Scm}^{-1}$
7	32 °C	$3.48 \times 10^{-3} \text{ Scm}^{-1}$	30 °C	$2.12 \times 10^{-4} \text{ Scm}^{-1}$

Table S4: High temperature proton conductivity of In-IA-2D-1 and -2 :

Sr. no	In-IA-2D-1		In-IA-2D-2	
	Temperature	Proton conductivity value (98% RH)	Temperature	Proton conductivity value (98% RH)
10	32 °C	$3.48 \times 10^{-3} \text{ Scm}^{-1}$	33 °C	$1.58 \times 10^{-4} \text{ Scm}^{-1}$
11	39 °C	$5.02 \times 10^{-4} \text{ Scm}^{-1}$	37 °C	$1.31 \times 10^{-4} \text{ Scm}^{-1}$
12	47 °C	$8.3 \times 10^{-5} \text{ Scm}^{-1}$	41 °C	$9.8 \times 10^{-5} \text{ Scm}^{-1}$
13	57 °C	$2.13 \times 10^{-5} \text{ Scm}^{-1}$	45 °C	$8.16 \times 10^{-5} \text{ Scm}^{-1}$
14	65 °C	$9.33 \times 10^{-6} \text{ Scm}^{-1}$	49 °C	$7.16 \times 10^{-5} \text{ Scm}^{-1}$
15			53 °C	$6.19 \times 10^{-5} \text{ Scm}^{-1}$
16			57 °C	$5.49 \times 10^{-5} \text{ Scm}^{-1}$
17			61 °C	$4.93 \times 10^{-5} \text{ Scm}^{-1}$
18			65 °C	$4.46 \times 10^{-5} \text{ Scm}^{-1}$
19			69 °C	$4.08 \times 10^{-5} \text{ Scm}^{-1}$
20			73 °C	$3.73 \times 10^{-5} \text{ Scm}^{-1}$
21			77 °C	$3.45 \times 10^{-5} \text{ Scm}^{-1}$
22			81 °C	$3.24 \times 10^{-5} \text{ Scm}^{-1}$
23			85 °C	$3.00 \times 10^{-5} \text{ Scm}^{-1}$
24			89 °C	$2.77 \times 10^{-5} \text{ Scm}^{-1}$
25			93 °C	$2.55 \times 10^{-5} \text{ Scm}^{-1}$
26			97 °C	$2.38 \times 10^{-5} \text{ Scm}^{-1}$
27			101 °C	$2.22 \times 10^{-5} \text{ Scm}^{-1}$
28			105 °C	$2.08 \times 10^{-5} \text{ Scm}^{-1}$
29			109 °C	$1.95 \times 10^{-5} \text{ Scm}^{-1}$
30			113 °C	$1.87 \times 10^{-5} \text{ Scm}^{-1}$
31			117 °C	$1.77 \times 10^{-5} \text{ Scm}^{-1}$
32			120 °C	$1.59 \times 10^{-5} \text{ Scm}^{-1}$

Table S5: Anhydrous proton conductivity of In-IA-2D-2 at variable temperatures:

The “anhydrous condition” refers to perfectly anhydrous system both from sample as well as proton conductivity chamber point of view. We have enclosed the sample holder in a dry N₂ containing chamber with occasional flushing of dry N₂ to ensure complete humid free environment throughout the measurements. The reproducibility of the entire process were confirmed by repeated experiments

In-IA-2D-2 (anhydrous condition)		
Serial. no	Temperature (°C)	Proton conductivity value (Anhydrous Condition)
1	25 °C	$2.61 \times 10^{-5} \text{ Scm}^{-1}$
2	40 °C	$2.56 \times 10^{-5} \text{ Scm}^{-1}$
3	55 °C	$2.12 \times 10^{-5} \text{ Scm}^{-1}$
4	60 °C	$2.51 \times 10^{-5} \text{ Scm}^{-1}$
5	77 °C	$2.72 \times 10^{-5} \text{ Scm}^{-1}$
6	80 °C	$1.37 \times 10^{-5} \text{ Scm}^{-1}$
7	90 °C	$1.18 \times 10^{-5} \text{ Scm}^{-1}$

Combined figures of wide range proton conductivity for In-IA-2D-1 :

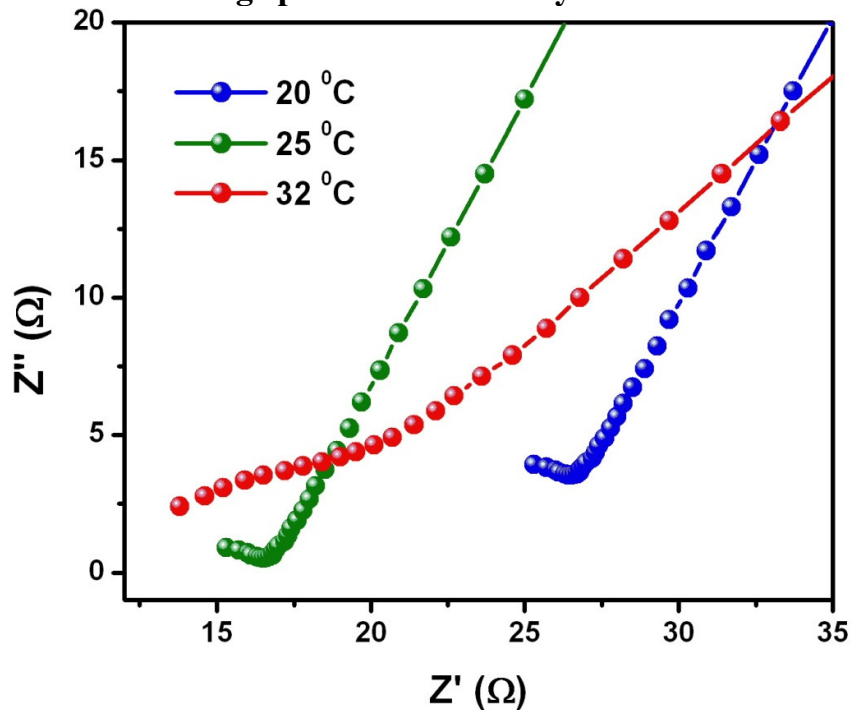


Figure S23: Proton conductivity plots of In-IA-2D-1 at lower temperature under 98% RH showing decrease in proton conductivity.

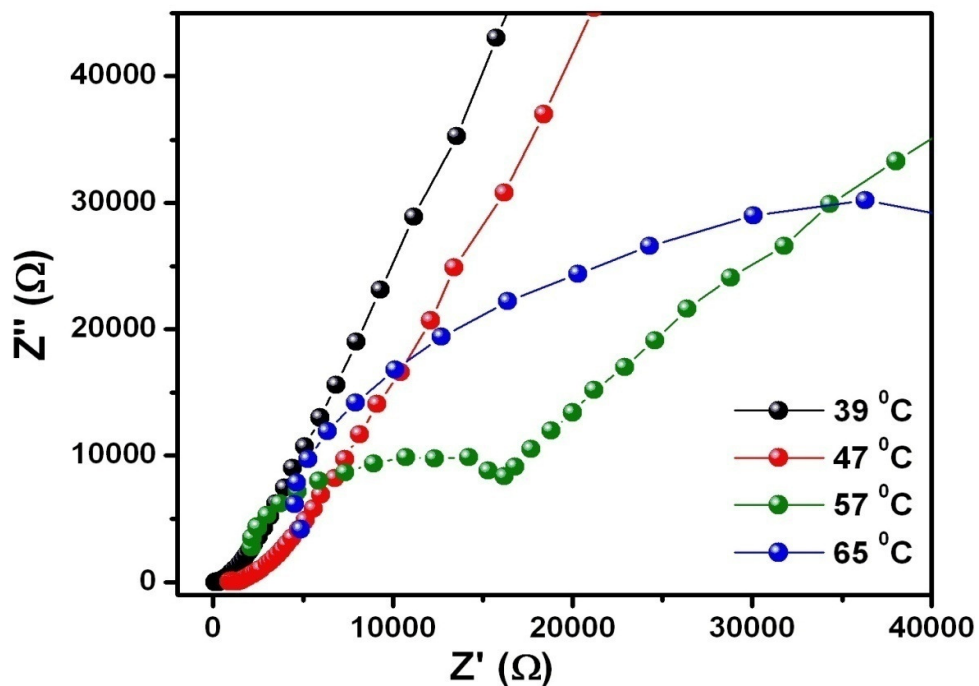


Figure S24: Proton conductivity plots of In-IA-2D-1 at elevated temperature under 98% RH showing decrease in proton conductivity values.

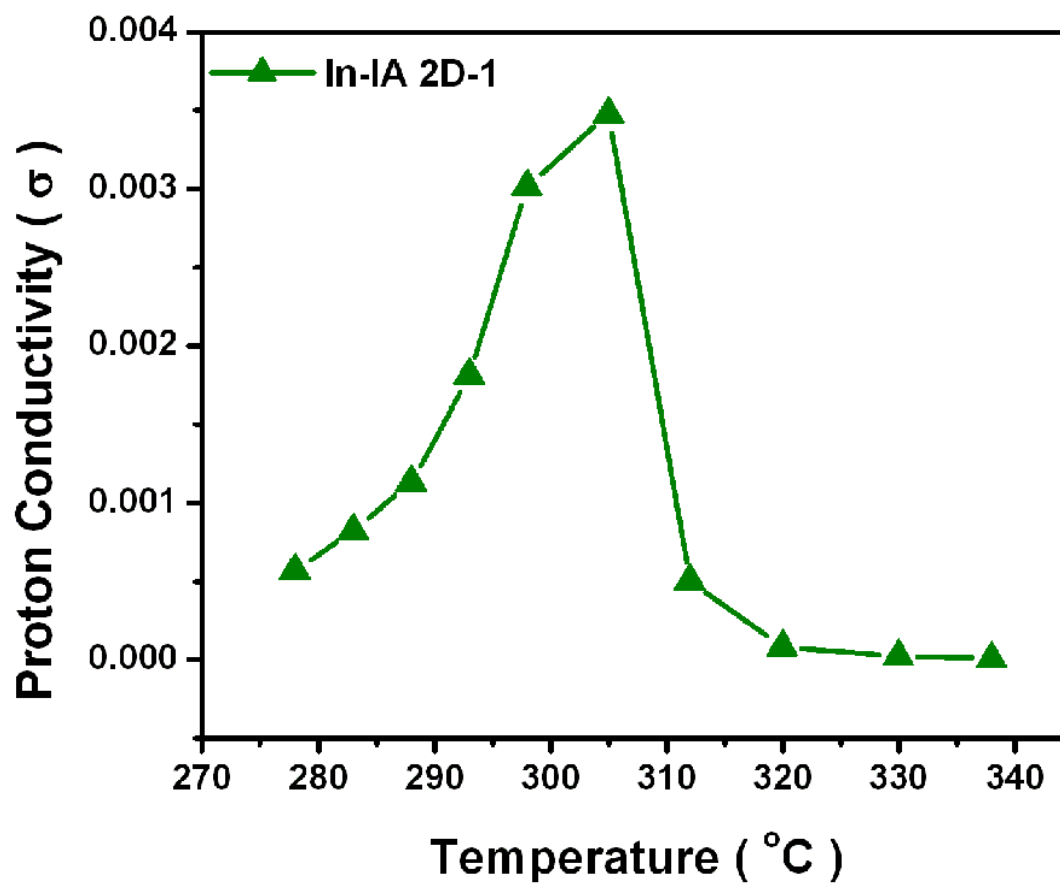


Figure S25: Proton conductivity Vs temperature plot of In-IA-2D-1 with increasing temperature under 98% RH.

Combined figures of wide range proton conductivity for In-IA-2D-2 :

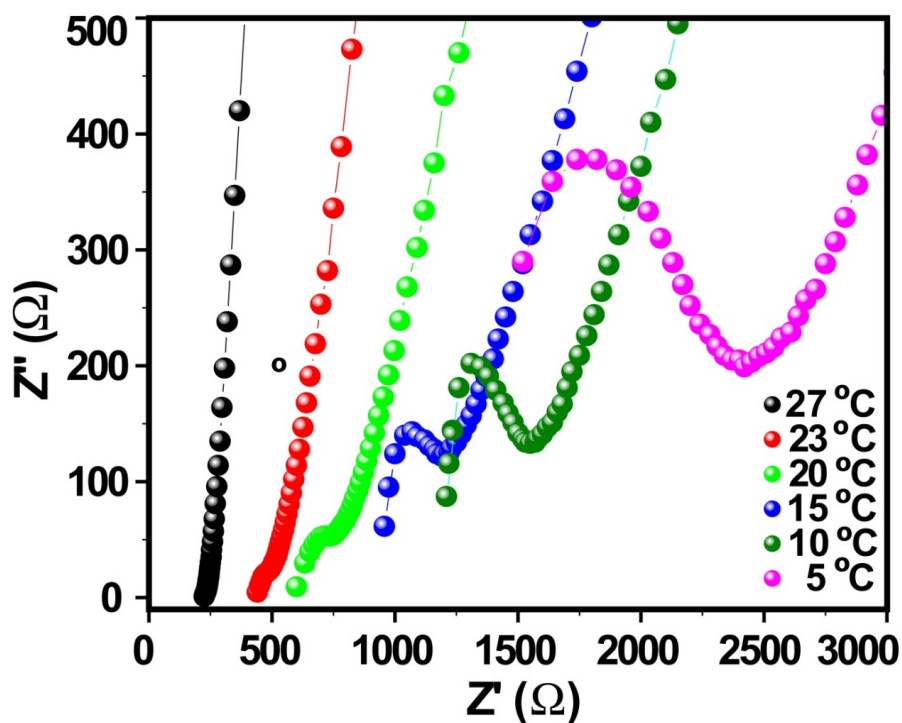


Figure S26: Proton conductivity plots of In-IA-2D-2 at lower temperature under 98% RH showing decrease in proton conductivity values.

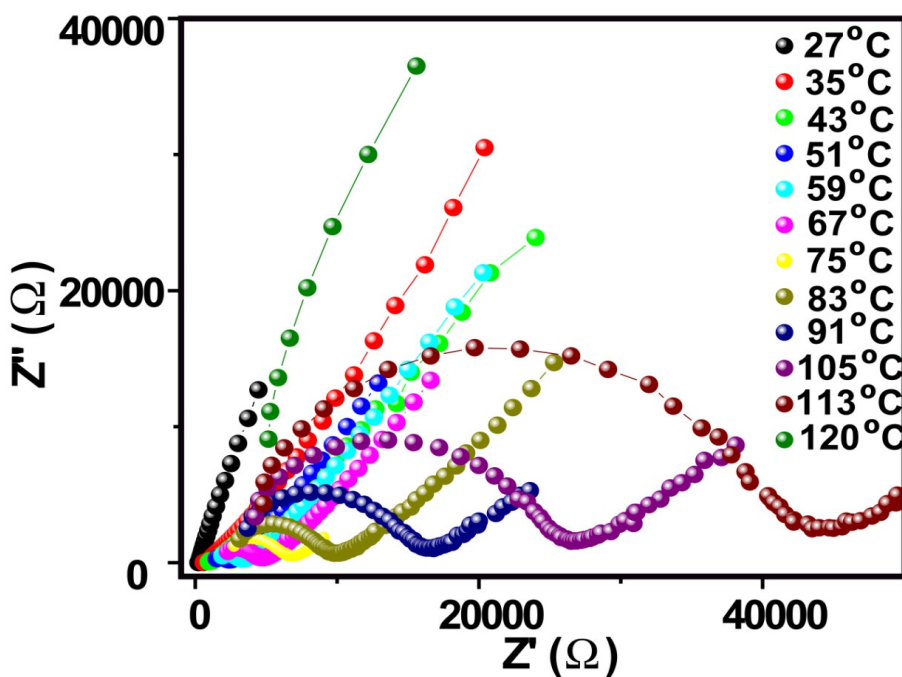


Figure S27: Proton conductivity plots of In-IA-2D-2 at elevated temperature under 98% RH showing decrease in proton conductivity values.

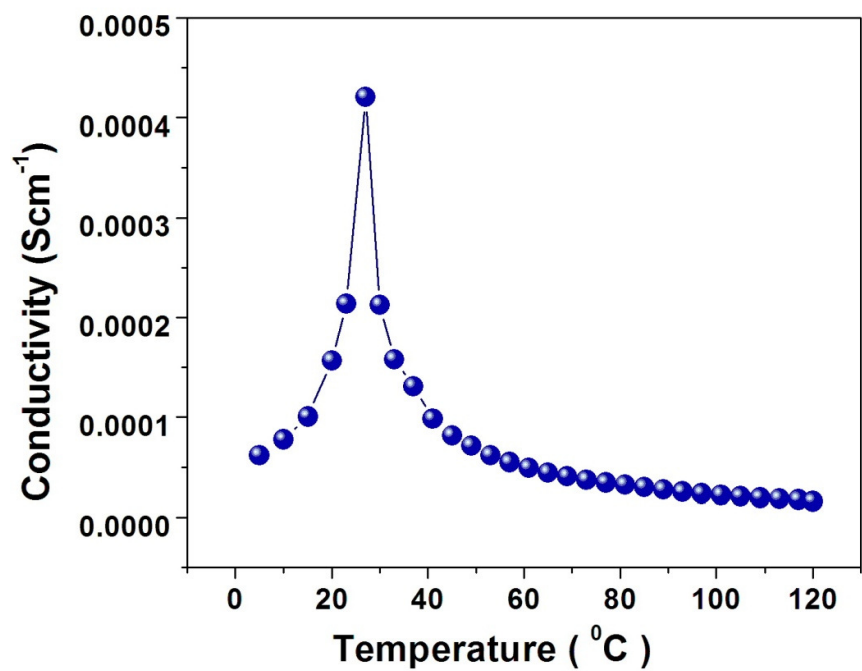


Figure S28: Proton conductivity vs temperature plot of In-IA-2D-2 under 98% RH.

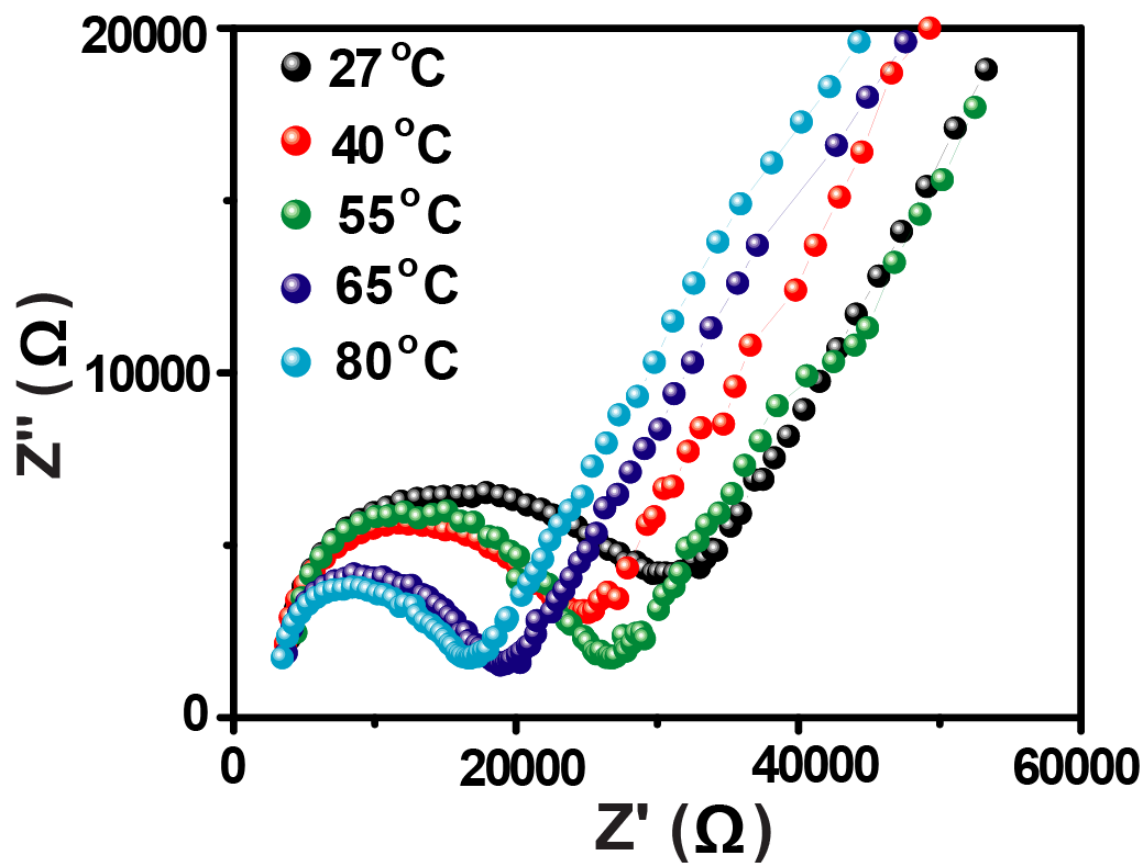


Figure S29: Anhydrous proton conductivity plots of In-IA-2D-2 at different temperatures.

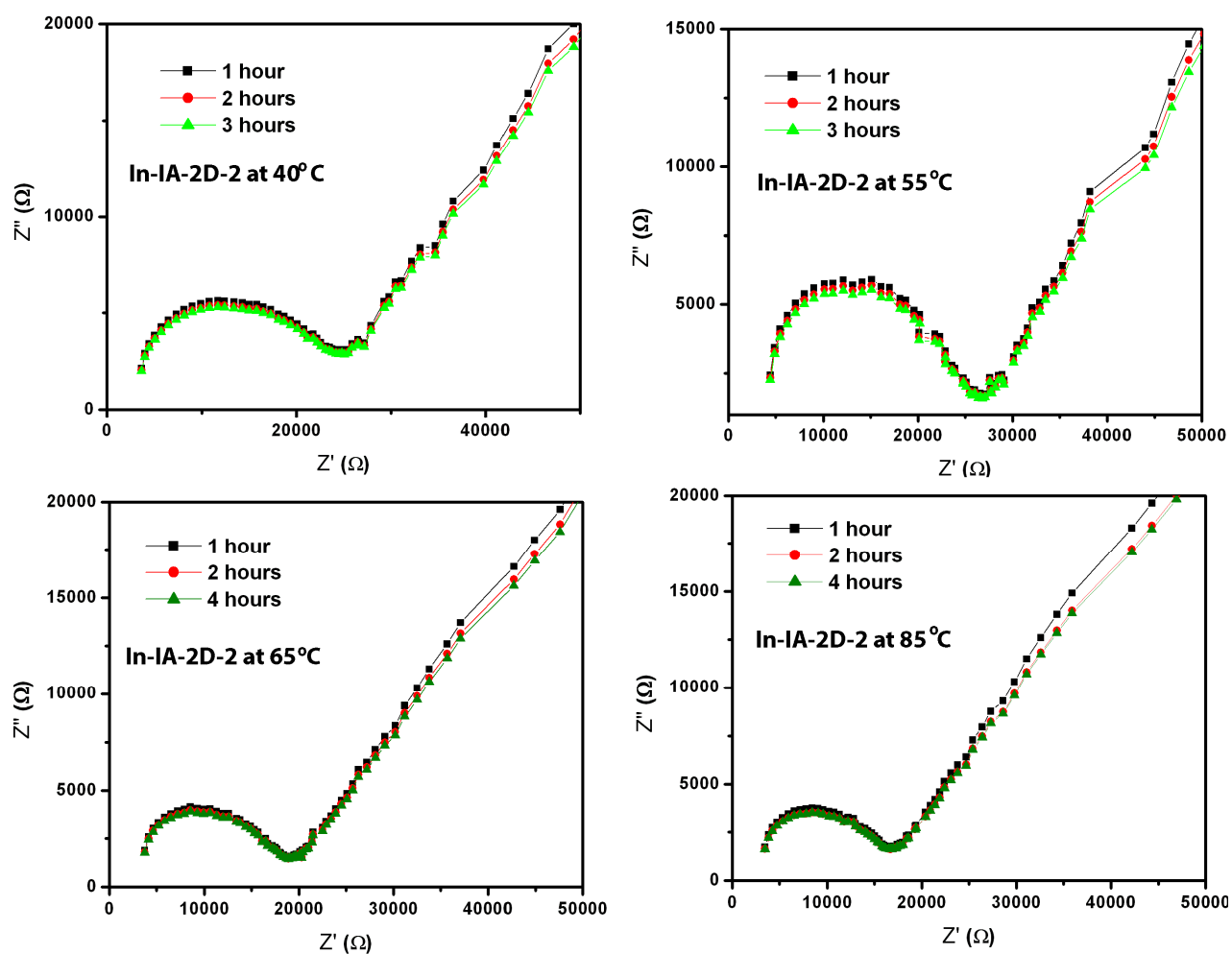


Figure S30: Anhydrous proton conductivity plots of In-IA-2D-2 at different temperatures (40, 55, 65 85 °C) for 1, 2 and 4 hrs respectively.

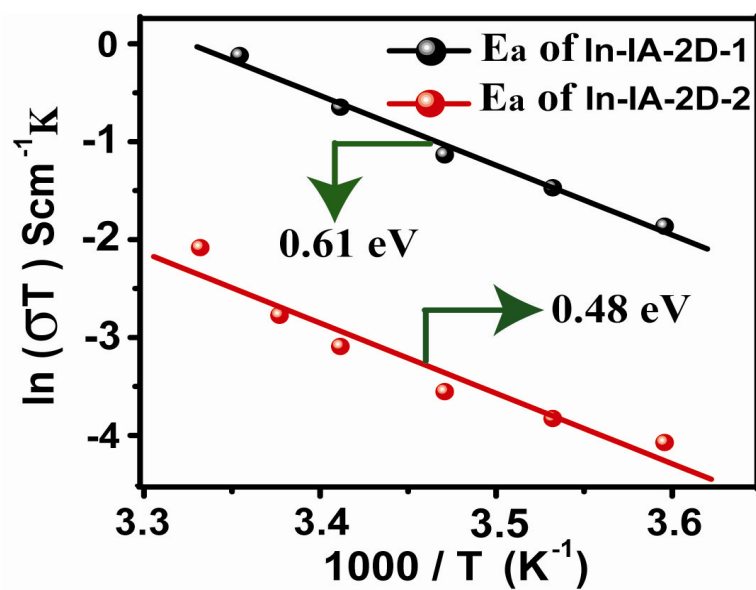


Figure S31: Arrhenius plot of activation energy (under 98% RH) for In-IA-2D-1 and -2 MOFs.

Humidity dependent proton conductivity of In-IA-2D-1 :

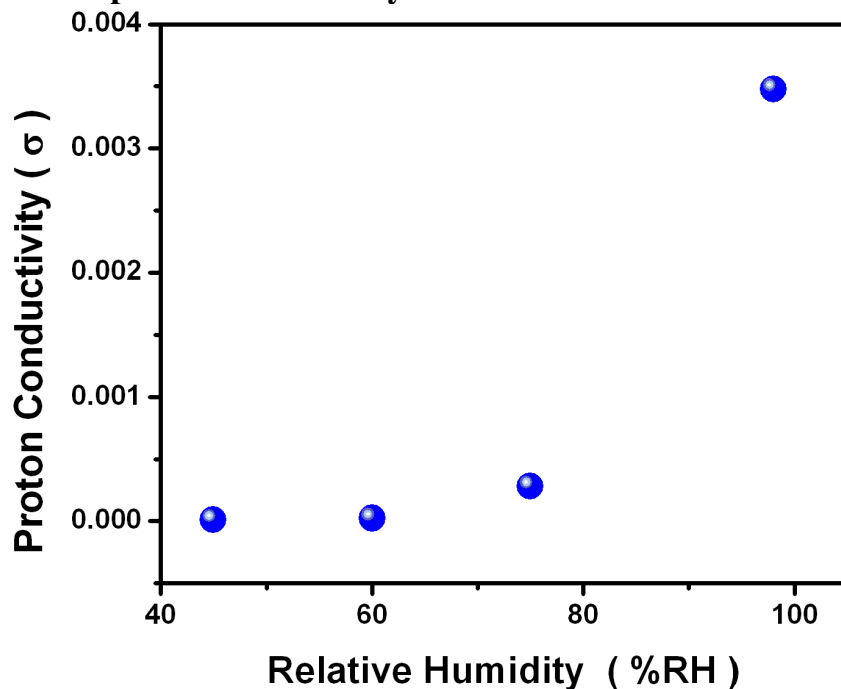


Figure S32: Proton conductivity vs relative humidity plot of In-IA-2D-1 at lesser humidity showing decrease in proton conductivity values.

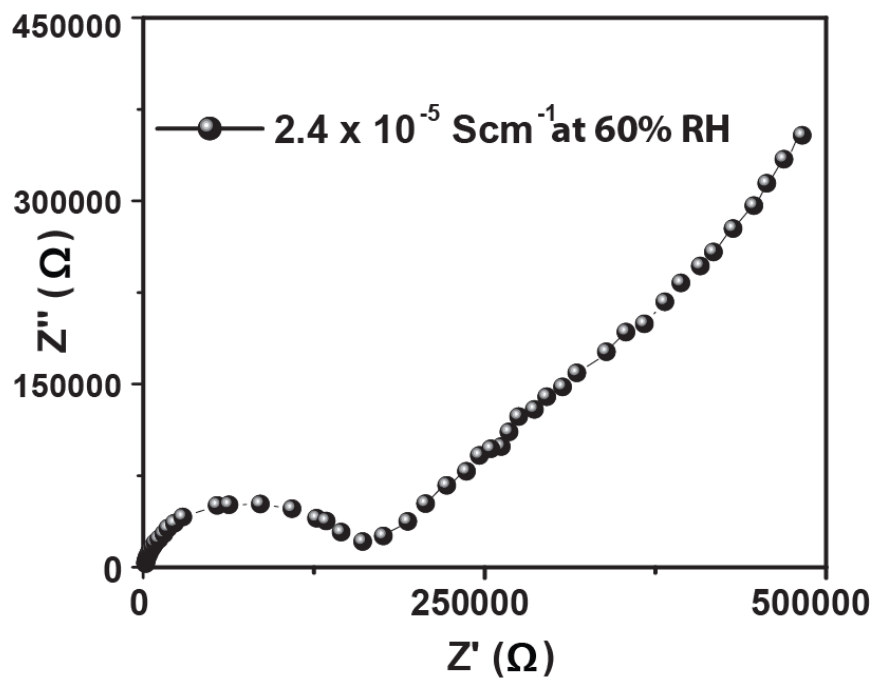


Figure S33: Proton conductivity plots of In-IA-2D-1 at lesser humidity (60% RH) showing decrease in proton conductivity values $2.4 \times 10^{-5} \text{ Scm}^{-1}$.

Humidity dependent proton conductivity of In-IA-2D-2 :

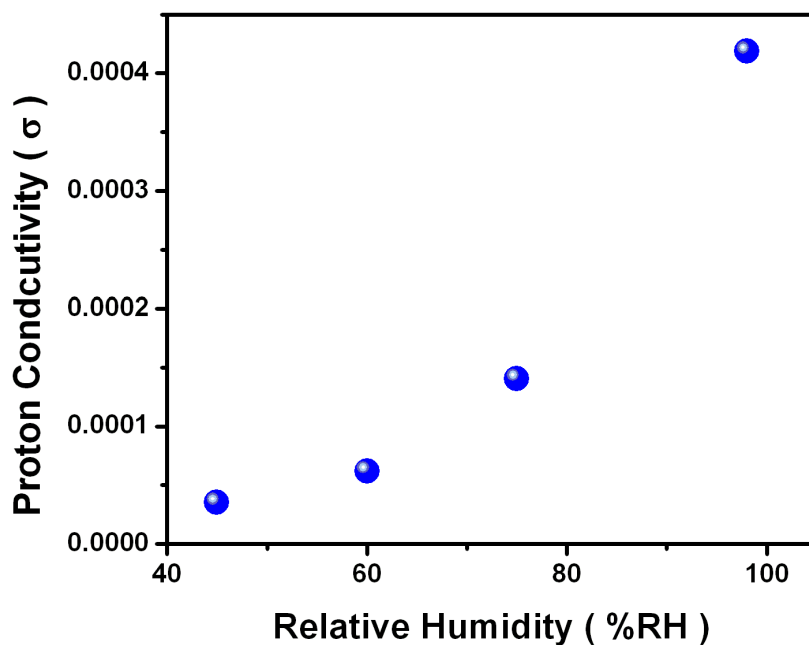


Figure S34: Proton conductivity vs relative humidity plot of In-IA-2D-2 at lesser humidity showing decrease in proton conductivity values.

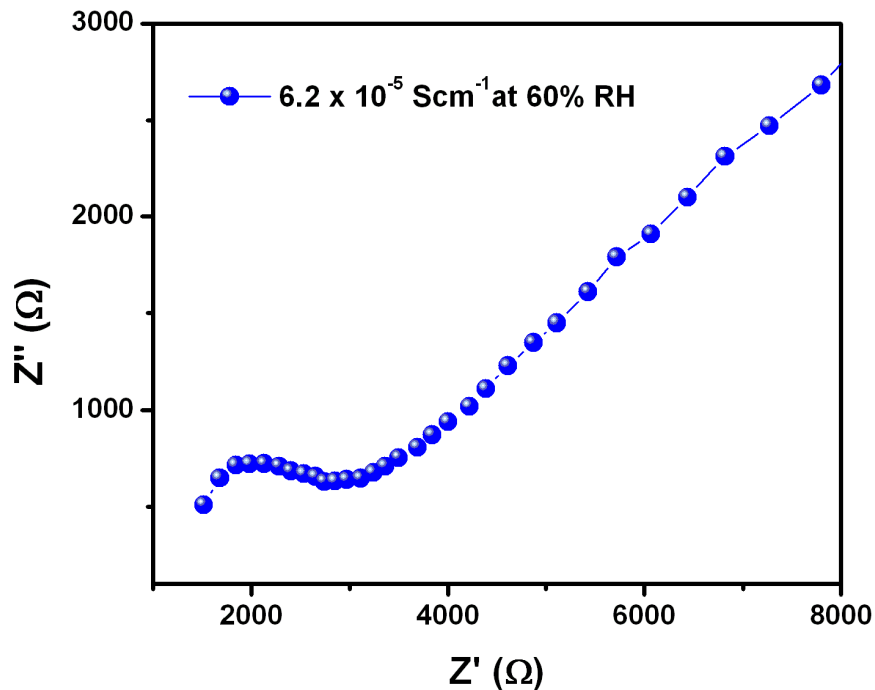


Figure S35: Proton conductivity plots of In-IA-2D-2 at lesser humidity (60% RH) showing decrease in proton conductivity values $6.2 \times 10^{-5} \text{ Scm}^{-1}$.

N.B. The proton conductivity vs humidity plots clearly shows proton conductivity increases with increasing humidification. We speculate that loosely bound water molecules due to humidification and dimethyl ammonium cations play a pivotal role in drastic difference in proton conductivity in these materials.

Table S6: Comparison of proton conductivity values of In-IA-2D-1 and -2 with other proton conducting MOF:

SL.No.	MOFs and CPs	Proton conductivity (S cm ⁻¹)	Ea value (eV)	Conditions	Reference
1	H ₂ SO ₄ @MIL-101	1 × 10 ⁻²	0.42	150 °C and 0.13 % RH	<i>J. Am. Chem. Soc.</i> DOI:, 10.1021/ja305587n
2	H ₃ PO ₄ @MIL-101	3 × 10 ⁻³	0.25	150 °C and 0.13 % RH	<i>J. Am. Chem. Soc.</i> DOI:, 10.1021/ja305587n
3	(NH ₄) ₂ (adp)[Zn ₂ (ox) ₃] · 3H ₂ O	8 × 10 ⁻³	0.63	25 °C and 98% RH	<i>J. Am. Chem. Soc.</i> 2009, 131, 9906
4	Cd-5TIA	3.6 × 10 ⁻³	0.163	28 °C and 98% RH	<i>Chem commun</i> 2012, 48, 5464
5	In-IA-2D-1	3.48 × 10 ⁻³	0.61	32 °C and 98% RH	<i>This Work</i>
6	MgH ₆ ODTMP·6H ₂ O	1.6 × 10 ⁻³	0.31	19 °C and 100% RH	<i>Inorg. Chem.</i> 2012, 51, 7689
7	1D Ferrous Oxalate Dihydrate	1.3 × 10 ⁻³	0.37	25 °C and 98% RH	<i>J. Am. Chem. Soc.</i> 2009, 131, 3144.
8	(NH ₄) ₄ [MnCr ₂ (ox) ₆] ₃ · 4H ₂ O.	1.1 × 10 ⁻³	0.23	25 °C and 98% RH	<i>J. Am. Chem. Soc.</i> ASAP 2011, 10.1021/ja206917z
9	Cucurbit[6]uril (CB[6])	1.1 × 10 ⁻³	0.39	25 °C and 98% RH	<i>Angew. Chem. Int. Ed.</i> 2011, 50, 7870.
10	(b-PCMOF2(Tz) _{0.45})	5 × 10 ⁻⁴	0.51	150 °C	<i>Nat. Chem.</i> 2009, 1, 705
11	In-IA-2D-2	4.2 × 10 ⁻⁴	0.48	32 °C and 98% RH	<i>This Work</i>
12	Mg ₂ (dobdc) ₃ ·0.35LiOiPr ₃ ·0.25LiBF ₄ ·EC3·DEC	3.1 × 10 ⁻⁴	0.14	27 °C	<i>J. Am. Chem. Soc.</i> 2011, 133, 14522
13	{NH(prol)3}[MIIICrIII(ox)3] (MII) =MnII, FeII, CoII)	1 × 10 ⁻⁴		25 °C and 75% RH	<i>J. Am. Chem. Soc.</i> , 2009, 131, 13516
14	(H ₅ C ₂) ₂ (dtoa) Cu	1 × 10 ⁻⁴		25 °C and 80% RH	<i>Bull. Chem. Soc. Jpn.</i> 2010, 83, 42
15	In-5TIA	5.35 × 10 ⁻⁵	0.137	28 °C and 98% RH	<i>Chem commun</i> 2012, 48, 5464
16	[Zn(l-LCl)(Cl)](H ₂ O) ₂	4.45 × 10 ⁻⁵	0.34	28 °C and 98% RH	<i>J. Am. Chem. Soc.</i> , 2011, 133, 17950
17	PCMOF-3	3.5 × 10 ⁻⁵	0.17	25 °C and 98% RH	<i>J. Am. Chem. Soc.</i> 2010, 132, 14055.

Section S7. Solid state NMR and I-V profile

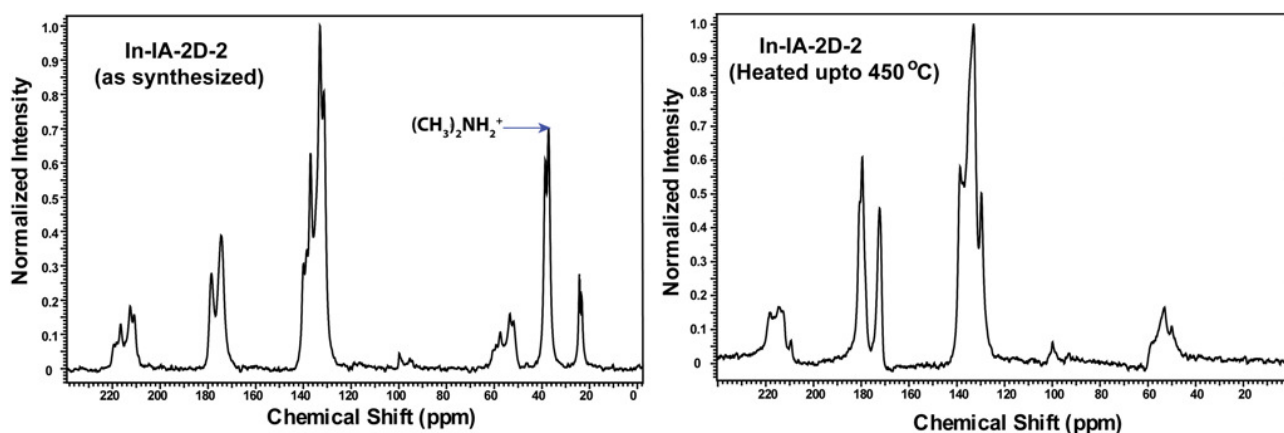


Figure S36. ^{13}C solid state NMR of In-IA-2D-2 sample as synthesized and 450 °C heated sample.

^{13}C solid state NMR of as synthesized In-IA-2D-2 shows there are peaks at 35.3 and 20 which correspond to the dimethyl ammonium cations and solvent ethanol molecules respectively. However, when we heated the sample of In-IA-2D-2 at 450 °C and then measured ^{13}C solid state NMR of In-IA-2D-2 we could not achieve to locate the peaks correspond to dimethyl ammonium cations as well as solvent ethanol molecules although the peaks correspond to framework molecules are intact like as synthesized molecule. Hence we anticipate that, at 450 °C the framework of In-IA-2D-2 is stable by removing dimethyl ammonium cations which eventually matches with the proton conductivity result as well as TGA profile of In-IA-2D-2.

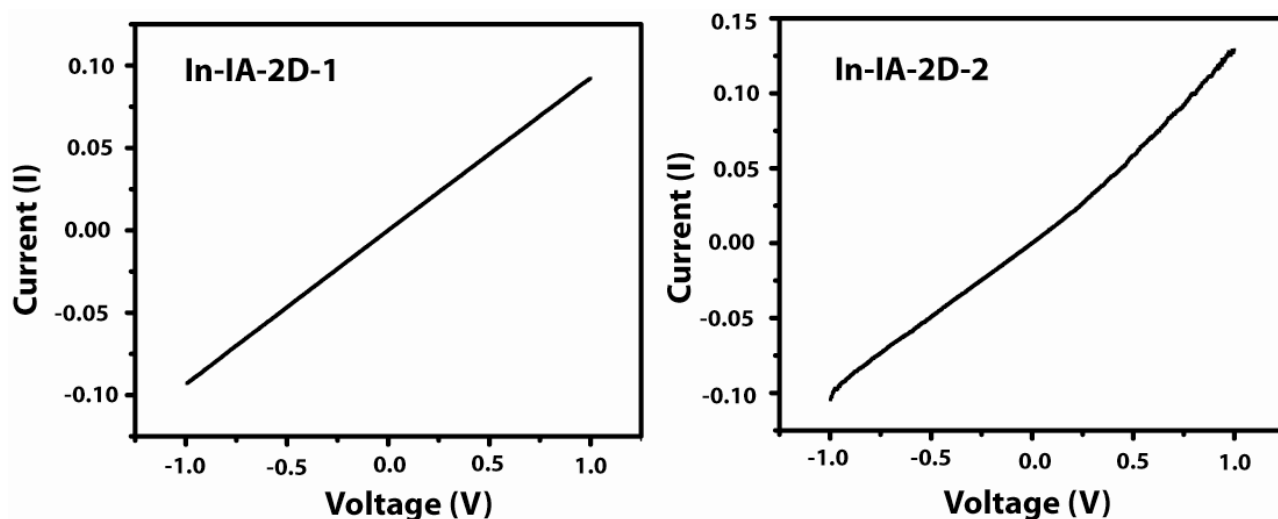


Figure S37. I-V profile diagram of In-IA-2D-1 and -2. It is interesting to note that, both In-IA-2D-1 and -2 are highly resistive and shows Ohmic behavior (Figure S37 in SI) which indicates they have no electrical conductivity.